

The quantum characteristics and structure of low-lying levels of the ^{10}Li nucleus

S. N. Abramovich, B. Ya Guzhovskii,⁽¹⁾ and L. M. Lazarev

Russian Federal Nuclear Center, All-Russian Institute of Experimental Physics, Arzamas-16

Fiz. Élem. Chastits At. Yadra **26**, 1001–1045 (July–August 1995)

The experimental results on the properties of low-lying states of the ^{10}Li nucleus are reviewed, together with theoretical methods of calculating the levels of light nuclei. The method of the theory of threshold phenomena has been used to analyze the two lowest states of the ^{10}Be nucleus with $T=2$ near the threshold of the reaction $^7\text{Li}(t,n)^9\text{Be}^*(T=3/2)$; these two states are the analogs of the ground and first excited states of ^{10}Li . The mass excesses of these ^{10}Li states and the $^{10}\text{Li} \rightarrow n + ^9\text{Li}$ decay energy are determined. The spins and parities of these states are found to be $J^\pi = 2^-, 1^-$, and their configuration is $\nu 2s_{1/2}$. The total widths are also estimated. The results are compared with the corresponding experimental and theoretical results of other studies. This analysis makes it possible to resolve the contradictions in the available experimental data by interpreting them correctly. The properties of nuclei of the $A=10$ isobaric multiplet are discussed. The systematics of nuclei with $N=7$ ($Z=0-6$) are studied and used to predict the spins and parities of the lowest states of the ^9He , ^8H , and ^7n nuclei with normal and anomalous parities. New experiments on more extensive study of the properties of ^{10}Li are also proposed. © 1995 American Institute of Physics.

INTRODUCTION

In the last few decades light exotic nuclei with $N/Z > 1$ have been studied intensively. The unusual behavior of these nuclei begins to be manifested at $N/Z \approx 2$, where a deviation from the shell-model level-filling scheme is seen, for example, for ^{11}Be . A neutron “halo” and associated anomalously large radius are seen in nuclei with $N/Z \approx 3$ (^8He , ^{11}Li). For $N/Z \approx 2.5$ (the ^{10}Li nucleus) the nuclear structure is that of a core ($A-1$) in the ground state plus a weakly bound extra neutron. This incomplete list of formerly unknown nuclear properties indicates that nuclear-physics research has entered a region of nuclei with new properties. This probably began with the publication of Ref. 1 in 1966 on the fragmentation of the uranium nucleus induced by 5.3-GeV protons, which led to the detection of nuclei of isotopes of light elements. In particular, the peak corresponding to ^{10}Li was not seen in the spectrum of these nuclei, from which it was concluded that ^{10}Li is unstable to the emission of nucleons or nucleon associations. Further research has confirmed this conclusion. The neutron instability of ^{10}Li is now considered an established fact.

In 1969 at a nuclear-isospin conference Barnes² presented results on the measurement of the excitation function of the reaction $^7\text{Li}(^3\text{He},p)^9\text{Be}$ near the $n + ^9\text{B}^*$ threshold ($E_x = 14.66$ MeV, $J^\pi = \frac{3}{2}^-, T=3/2$). The proposed level of the compound nucleus near the neutron threshold must have a large reduced neutron decay width and isospin $T=2$, corresponding to structure of the ^{10}B nucleus of the form of a core $^9\text{B}^*(T=3/2)$ and a neutron in an outer orbital. This state of ^{10}B is the analog of the ^{10}Be state with structure $n + ^9\text{B}^*(E_x = 14.3922$ MeV, $J^\pi = \frac{3}{2}^-, T=3/2$) and of the ^{10}Li state with structure $n + ^9\text{Li}$ ($J^\pi = \frac{3}{2}^-, T=3/2$). The core must be in the ground state, since the ^{10}B level in question is the lowest of the levels with $T=2$. Studies soon appeared in which the excitation functions of the reactions $T(^7\text{Li},p)^9\text{Li}$ (Ref. 3) and $^7\text{Li}(t,p)^9\text{Li}$ (Refs. 4 and 5) were measured near

the neutron threshold $n + ^9\text{Be}^*(E_x = 14.39$ MeV, $J^\pi = \frac{3}{2}^-, T=3/2$), and the level of the compound nucleus $^{10}\text{Be}(T=2)$ which is the analog of the ground state of ^{10}Li was found. In Ref. 5 the orbital angular momentum of threshold neutrons was found to be $l=0$. This result was unexpected, because it leads to negative parity of the analog state $^{10}\text{Be}(T=2)$ and of the ground state of ^{10}Li . According to the calculations based on the shell model,⁶ these states should have positive parity. A mass excess of the ^{10}Li nucleus equal to 33 MeV was found from the energy of the analog state.⁷

However, in 1975 in an experiment using the reaction $^9\text{Be}(^9\text{Be},^8\text{B})^{10}\text{Li}$ (Ref. 8), it was found that the ^{10}Li mass excess is 33.83 ± 0.25 MeV and that the parity is positive. This discrepancy between the data of Refs. 4 and 5 and Ref. 8 led to discussions about the ground-state configuration of ^{10}Li (Ref. 9) and stimulated shell-model calculations of the levels of light nuclei far from stability.¹⁰ In Ref. 9 the shell-model calculations¹¹ were used as the basis for proposing that the authors of Ref. 8 had observed the ^{10}Li nucleus in the lowest excited state with normal (positive) parity. The ground state of ^{10}Li apparently has the configuration $1s^4 1p^5 2s$ and lies 0.8 MeV below the state observed in Ref. 8.

Later experimental studies focused on improving the values of the ^{10}Li mass excess and the spin and parity of its ground and excited states. The results of Refs. 4 and 5 were confirmed in Ref. 12. The authors of Refs. 13–15 did not draw any definite conclusions about the ^{10}Li ground state, owing to insufficient statistics. Finally, in Ref. 16, where ^{10}Li was studied in two different reactions, $^9\text{Be}(^{13}\text{C}, ^{12}\text{N})^{10}\text{Li}$ and $^{13}\text{C}(^{14}\text{C}, ^{17}\text{F})^{10}\text{Li}$, it was confirmed that the ^{10}Li nucleus is particle-unstable and has levels above the neutron threshold with energies 0.42 and 0.8 MeV, which with highest probability are identified as the $1^+/2^+$ doublet with the configuration $[\pi 1p_{3/2} \otimes \nu 1p_{1/2}]$, where the 1^+ state is the ground state. This last statement contradicts the available experimental data, as well as the theoretical analysis^{17,18} of the excitation

function of the reaction ${}^7\text{Li}(t,p){}^9\text{Li}$ (Refs. 4 and 5).

The resolution of this complicated situation requires a unified approach to the experimental data and a key to understanding them. The tools available to us are the model-independent theory of threshold phenomena, which allows a unified interpretation of the available data on ${}^{10}\text{Li}$, and also precise experimental data on the two lowest levels of ${}^{10}\text{Be}$ with isospin $T=2$, which are the analogs of the ground and first excited states of ${}^{10}\text{Li}$ and have been used to find an approach to understanding the properties of the ${}^{10}\text{Li}$ levels. We resolved to use these tools to analyze the available data on the properties of the ground and excited states of ${}^{10}\text{Li}$ and to check that the experimental data are consistent. In 1994 we carried out a theoretical analysis of the experimental data of Ref. 20, where the energy resolution was 20 keV, the error was small ($<0.5\%$), and the point spread was insignificant. In contrast to the earlier analysis^{17,18} of other experimental data for the same reaction ${}^7\text{Li}(t,p){}^9\text{Li}$ near the threshold of the reaction ${}^7\text{Li}(t,n){}^9\text{Be}^*(E_x=14.3922\text{ MeV}, J^\pi=\frac{3}{2}^-, T=3/2)$, we discovered two (rather than one) narrow levels of the compound nucleus ${}^{10}\text{Be}$. The level widths are less than 100 keV, and both levels have negative parity. It was found that these levels have isospin $T=2$ and are the analogs of the ground and first excited levels of ${}^{10}\text{Li}$. We determined the energies and widths of these levels, and also estimated their neutron widths. The results led to a ${}^{10}\text{Li}$ mass excess in agreement with the data of Refs. 17 and 18. We were also able to find the energies and widths of the ground and first excited states of ${}^{10}\text{Li}$, and to determine their parity, structure, and shell configuration. These results later greatly simplified the analysis of the other experimental data.

In order to introduce the reader to the subject, first we review the experimental (Sec. 1) and theoretical (Sec. 2) studies with a detailed discussion of the results obtained on the properties of ${}^{10}\text{Li}$. We then present the theoretical analysis of the levels of ${}^{10}\text{Be}$ with $T=2$ (Sec. 3) and make an analog prediction for the properties of the ground and first excited states of ${}^{10}\text{Li}$. In Sec. 5 we discuss the results on the properties of ${}^{10}\text{Li}$ obtained by us and in other studies. In Sec. 6 we draw some conclusions and suggest experimental work to further improve our knowledge of the characteristics of ${}^{10}\text{Li}$ and the nuclei of the $A=10$ multiplet.

1. REVIEW OF THE EXPERIMENTAL DATA

The experimental results on the ${}^{10}\text{Li}$ nucleus can be divided into three groups: (1) data on nucleon-stable nuclei of the $A=10$ isobaric multiplet; (2) direct study of ${}^{10}\text{Li}$ in reactions producing this nucleus; and (3) indirect data, primarily data on the nuclei of neighboring multiplets with $A=11$ and $A=9$.

The data of the first group represent the most complete and accurate information available at present. We shall give special attention to them. Methods for studying ${}^{10}\text{Li}$ directly are not well developed, and their results cannot be interpreted unambiguously. Therefore, the data of the second group are still viewed as auxiliary. Information on other nuclei with $A \neq 10$ is used to construct several logical schemes which aid in the understanding of the ${}^{10}\text{Li}$ structure and its

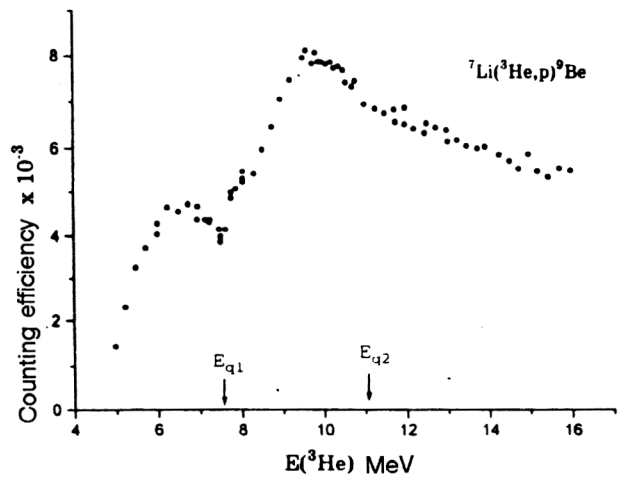


FIG. 1. Data on the yield of 14.5- and 12-MeV γ rays² from deexcitation of the lowest $T=3/2$ states of ${}^9\text{Be}$ and ${}^9\text{B}$ as a function of the energy of the incident ${}^3\text{He}$ nuclei for the reactions ${}^7\text{Li}({}^3\text{He},p){}^9\text{Be}$ ($T=3/2$) and ${}^7\text{Li}({}^3\text{He},n){}^9\text{B}$ ($T=3/2$). The two anomalies near the two thresholds E_{q1} and E_{q2} for ${}^9\text{B}$ ($T=3/2$) production are due to the isospin coupling between the two analog channels.

place among neighboring nuclei, and helps to extrapolate its properties to other nuclei.

(1) Data on $T=2$ levels of ${}^{10}\text{Be}$ and ${}^{10}\text{B}$ are presented in Refs. 2, 4, and 5. Reference 2 presents a figure from an unpublished study (by Addelberger and Snover of Stanford University) which shows the yield of γ quanta of energy 14.5 and 12 MeV from the lowest excited states of ${}^9\text{Be}$ and ${}^9\text{B}$ with $T=3/2$, produced in the reactions ${}^7\text{Li}+{}^3\text{He} \rightarrow p+{}^9\text{Be}$ ($T=3/2$) and ${}^7\text{Li}+{}^3\text{He} \rightarrow n+{}^9\text{B}$ ($T=3/2$) in the range of ${}^3\text{He}$ energies from 5 to 16 MeV (Fig. 1). At an energy near the neutron threshold of the reaction ${}^7\text{Li}({}^3\text{He},n){}^9\text{B}^*$ ($E_x=14.655\text{ MeV}$, $J^\pi=\frac{3}{2}^-, T=3/2$), $E_{q1}=7.577\text{ MeV}$, the threshold cusp is clearly seen, with two narrow resonances of the compound nucleus ${}^{10}\text{B}$ located to the left and right of it at $E_{q1} \pm 0.5\text{ MeV}$. Both resonances apparently have isospin $T=2$. For a bombarding energy near 10 MeV a strong resonance is observed which, as suggested by the authors of Ref. 2, might be the lowest $T=2$ state of the ${}^{10}\text{B}$ nucleus. In our opinion this strong resonance is either one of the $T=2$ levels or the giant resonance. On its right-hand slope at the energy corresponding to the second neutron threshold $E_{q2}=11.036\text{ MeV}$ of the reaction ${}^7\text{Li}({}^3\text{He},n){}^9\text{B}^*$ ($E_x=17.076\text{ MeV}$, $T=3/2$) we clearly see a second threshold cusp. It is quite likely that near this threshold, owing to correlations between threshold and resonance states,^{18,19} there are one or several levels of the compound nucleus ${}^{10}\text{B}$ with $T=2$. The next energy step in Ref. 2 is 150 keV, so that the detailed behavior of the excitation function is not seen in the experimental data.

The authors of Ref. 3 report on the measurement of the excitation function in the reaction $\text{T}({}^7\text{Li},p){}^9\text{Li}$ and the observation of a threshold singularity near the neutron threshold of the reaction $\text{T}({}^7\text{Li},n){}^9\text{Be}^*$ ($T=3/2$). The form of the excitation function is not given.

The most complete and accurate data on the lowest $T=2$

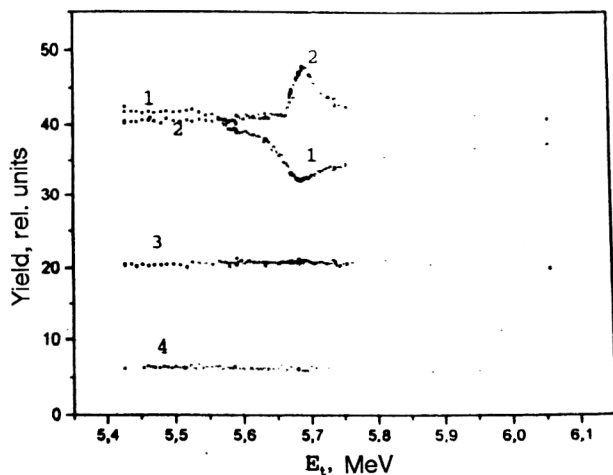


FIG. 2. Particle yields in various channels⁵ as a result of the reaction ${}^7\text{Li}+T$. Near the first threshold E_q of the reaction ${}^7\text{Li}(t,n){}^9\text{Be}^*$ ($E_x=14.39$ MeV, $T=3/2$) the excitation function of the channel ${}^9\text{Li}+p$ (1) has a complicated structure. The neutron yield (2) recorded by the threshold detector is constant up to the threshold energy E_q . The prethreshold yield comes from the detection of fast neutrons. The leading front of the threshold peak has a shape characteristic for zero orbital angular momentum of the threshold neutrons. Within the experimental error, no anomalies are observed in the yields of fast neutrons (3) and in the reaction ${}^7\text{Li}(t,\alpha){}^6\text{He}$ (4) near threshold.

levels of ${}^{10}\text{Be}$ were obtained in the experiments of Ref. 20, performed at the All-Russian Institute of Experimental Physics. The excitation function for the reaction ${}^7\text{Li}(t,p){}^9\text{Li}$ was studied in 1973 by measuring the activity of ${}^9\text{Li}$ nuclei undergoing β decay. The neutron and γ -ray background was 5% on the average. The excitation function was measured in the energy range $E_t=3.5$ –6 MeV with average energy step equal to 20 keV. Near the threshold of the reaction ${}^7\text{Li}(t,n){}^9\text{Be}^*(E_x=14.39$ MeV, $J^\pi=\frac{3}{2}^-$, $T=3/2$) at the energy $E_t=5.65$ MeV a giant threshold anomaly is observed (Fig. 2) with a 30% drop in the excitation function. The neutron threshold is located approximately at the center of the drop. The large value of the drop is explained by the existence in the charge-conjugate channel of a compound-nucleus state with $T=2$. The small energy width of the drop (≈ 0.1 MeV) is explained by the isospin-forbidden production of this state in the entrance channel, where this state is the analog of the state of the ${}^{10}\text{Li}$ nucleus. Analysis led to a value of 21.185 MeV for the energy of this state, and this was used to calculate the neutron binding energy $\epsilon_n=-62\pm 60$ keV in ${}^{10}\text{Li}$ for the ground state. The large spread of the experimental points in this study should be noted.

A more complete experiment⁵ was designed to study simultaneously the anomaly range $E_t=5.43$ –5.95 MeV in all the open channels of the reaction ${}^7\text{Li}+t$, except for the elastic channel. The data on the cross sections of the studied channels are given in Fig. 2. The excitation function of channels with nonthreshold neutrons does not have visible threshold singularities like that of the channel ${}^6\text{He}+\alpha$. This can be attributed to the weak coupling of these channels to the proton channel and the threshold channel. The latter have clearly expressed threshold singularities. Since the threshold-neutron detector was located on the beam axis behind the target, it received neutrons from nonthreshold channels and

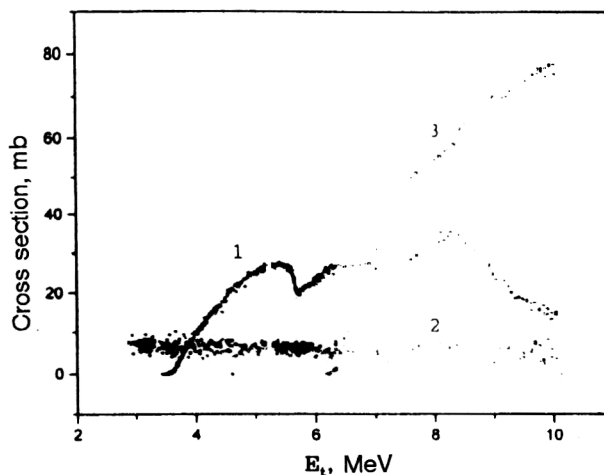


FIG. 3. Total cross sections of the reactions²⁰ ${}^7\text{Li}(t,p){}^9\text{Li}$ (1), ${}^7\text{Li}(t,\alpha){}^6\text{He}$ (2), and ${}^7\text{Li}(t,d){}^8\text{Li}$ (3). Threshold anomalies are observed only in the proton channel.

all threshold neutrons with energy in the range from zero to several times E_{max} , determined by the reaction kinematics and the angular dimensions of the detector. As the energy of the incident tritons is increased further, the number of threshold neutrons begins to fall, owing to opening of the “threshold” cone in which the neutrons travel, which forms the edge of the threshold cusp on the high-energy side. The height of the peak is 15% of the prethreshold yield. The shape of the left side of the peak is well described by a function of the energy $E_n^{l_n+1/2}$ with orbital angular momentum $l_n=0$. Therefore, the contribution of threshold neutrons with $l_n\neq 0$ is small. The total cross section of the ${}^9\text{Li}+p$ channel was measured according to the equilibrium β activity of the ${}^9\text{Li}$ nuclei directly in the bombardment process, i.e., in the stationary regime. For this reason the spread of the experimental points is minimal. The contribution of background effects is less than 1%. On the steep falloff of the excitation function we clearly see two bulges suggesting the existence of two narrow resonances of the compound nucleus ${}^{10}\text{Be}$. This study experimentally confirmed the suggestion⁴ that the decay to the threshold channel $n+{}^9\text{Be}^*(T=3/2)$ occurs with $l_n=0$. Therefore, if there is a state in ${}^{10}\text{Be}$ with $T=2$ and negative parity ($l_n=0$) near threshold, it will be manifested considerably more strongly than a state of positive parity ($l_n=1$).

The extension of the excitation function of the reaction ${}^7\text{Li}(t,p){}^9\text{Li}$ to the energy range $E_t=6$ –10.5 MeV was first obtained in Ref. 20. In Fig. 3 we show the total cross sections obtained in that study for ${}^6\text{He}$, ${}^8\text{Li}$, and ${}^9\text{Li}$ production in the reaction ${}^7\text{Li}+t$ as a function of energy in the range $E_t=3$ –10.5 MeV. The excitation function of the reaction ${}^7\text{Li}(t,p){}^9\text{Li}$ has a very complicated structure. After a fast rise from the threshold of the proton channel at about 5.65 MeV there is observed to be a sharp threshold anomaly due to the coupling to the channel $n+{}^9\text{Be}^*(E_x=14.39$ MeV, $T=3/2$). In the range 6–7.5 MeV the excitation function has a plateau behavior, followed by a broad peak with a maximum at $E_t=8.4$ MeV reaching a height of 35 mb. The resonance width is about 1 MeV. Then there is a rapid decrease down to the edge of the region studied. On this slope at $E_t=9.348$

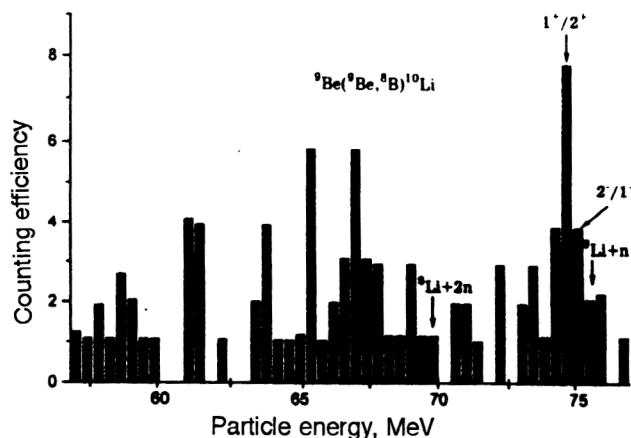


FIG. 4. Spectrum of ${}^8\text{B}$ nuclei from the reaction ${}^9\text{Be}({}^9\text{Be}, {}^8\text{B}){}^{10}\text{Li}$ at energy 121 MeV at an angle of 14° in the lab frame in coincidence with ${}^9\text{Li}$ nuclei (from the decay ${}^{10}\text{Li} \rightarrow {}^9\text{Li} + n$; Ref. 8). The broad peak with $\Gamma = 1.2 \pm 0.3$ MeV (c.m. frame) near the ${}^9\text{Li} + n$ threshold covers the two proposed level doublets $2^-/1^-$ and $1^+/2^+$ of the ${}^{10}\text{Li}$ nucleus.

MeV there is a second neutron threshold of the channel $n + {}^9\text{Be}^*$ ($E_x = 16.975$ MeV, $T = 3/2$) analogous to the first threshold. At the point corresponding to the threshold of the excitation function of the channel ${}^7\text{Li}(t, p){}^9\text{Li}$ we observe a discontinuity, and also the deep drop below the plateau at $E_t = 6-7.5$ MeV indicates the interaction of the threshold with a $T = 2$ level of ${}^{10}\text{Be}$. This level might be the strong resonance at $E_t = 8.4$ MeV or another state located on the decreasing side near the second neutron threshold. In Fig. 3 we also show the excitation functions of the reactions ${}^7\text{Li}(t, \alpha){}^6\text{He}$ and ${}^7\text{Li}(t, d){}^8\text{Li}$. The first was measured with a random error of $\approx 30\%$, and the only thing that can be said about it is that in the entire energy range $E_t = 3-10.5$ MeV the excitation function can be estimated to be roughly constant at ≈ 5 mb. The excitation function of the channel $d + {}^8\text{Li}$ grows monotonically from threshold in proportion to the Coulomb penetration factor and reaches a value of 75 mb at $E_t = 10.5$ MeV. The random errors in the channels $p + {}^9\text{Li}$ and $d + {}^8\text{Li}$ are determined by the counting statistics ($\leq 1\%$) and by the instrumental instability, leading to spreads of less than 3%. The total systematic error in the cross section is estimated to be 20%.

(2) Reactions with ${}^{10}\text{Li}$ production have been studied in Refs. 8 and 12–16. The mass excess of ${}^{10}\text{Li}$ was found to be 33.83 ± 0.25 MeV in 1975 for the reaction ${}^9\text{Be}({}^9\text{Be}, {}^8\text{B}){}^{10}\text{Li}$ at 121 MeV (Fig. 4). This corresponds to the binding energy of a neutron in ${}^{10}\text{Li}$ equal to 0.80 ± 0.25 MeV, which is considerably larger than the prediction of 0.21 MeV based on the Garvey–Kelson method,²¹ and is in even greater conflict with the data of Abramovich *et al.*,⁴ where it is only 0.062 ± 0.060 MeV. In Ref. 9 it was suggested that the ${}^{10}\text{Li}$ level observed in Ref. 8 is the lowest level with positive parity, and not the ground state with anomalous (negative) parity lying 0.8 MeV lower.

The spectrum of protons from the reaction ${}^{11}\text{B}(\pi^-, p){}^{10}\text{Li}$ induced by stopped π^- mesons was measured in Ref. 12. Near the upper kinematic limit the spectrum has a peak (Fig. 5) with the parameters $E_r = 0.15 \pm 0.15$ MeV and $\Gamma_0 < 0.4$

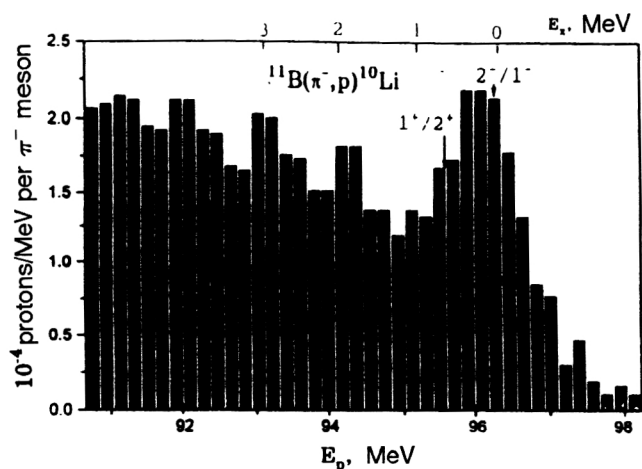


FIG. 5. Spectrum of protons from the reaction ${}^{11}\text{B}(\pi^-, p){}^{10}\text{Li}$ on stopped π^- mesons near the kinematic limit. The ${}^{10}\text{Li}$ excitation energy is shown on the upper scale. The arrows indicate the locations that we propose for the centroids of the ${}^{10}\text{Li}$ level doublets with negative and positive parities.

MeV, where $\Gamma = \Gamma_0(E/E_r)^{1/2}$. The spectrum taking into account the threshold nature of the ${}^{10}\text{Li}$ resonance was described by the Breit–Wigner formula with energy dependence of the width in the s -wave approximation ($l=0$). The absence of additional peaks in the proton spectrum can be due either to the reaction dynamics or to the fact that the distance between levels is considerably less than 0.4 MeV.

In the last two years a great advance has been made in the study of the properties of ${}^{10}\text{Li}$ in several laboratories around the world. The experimental data from Japan¹³ on the reaction ${}^{11}\text{Li} + \text{C} \rightarrow {}^9\text{Li} + n + X$ for $E({}^{11}\text{Li}) = 72$ MeV/A were obtained for the spectrum of neutrons in coincidence with ${}^9\text{Li}$. The observed distribution decreases monotonically from threshold and has a broad peak at 0.5 MeV. The three narrower peaks on it correspond to the data of Refs. 12, 16, and 8. The authors suggest that the ground state of ${}^{10}\text{Li}$ is slightly lower than in Ref. 12. There is also a hint of the first excited state near the same energy as in Ref. 16. These results suggest that the outer neutron in ${}^{10}\text{Li}$ can be in the $s_{1/2}$ shell.

In the United States, Young *et al.*¹⁴ have measured the spectrum of ${}^8\text{B}$ from the reaction ${}^{11}\text{B}({}^7\text{Li}, {}^8\text{B}){}^{10}\text{Li}$ at energy 130 MeV and laboratory angles 5° and 3.5° (Fig. 6). There is a strong, broad peak ($\Gamma_{\text{lab}} = 358 \pm 23$ keV) corresponding to the p -wave resonance in the interaction of the unbound neutron with ${}^9\text{Li}$ at 538 ± 62 keV. There is also a weak indication that the ground state can be either an s - or a p -wave resonance with $\Gamma_{\text{lab}} < 230$ keV corresponding to $\epsilon_n \geq -100$ keV. The clear splitting of the weak resonance into two should be noted.

Another American study¹⁵ focused on coincidences of n and ${}^9\text{Li}$ from the decay of ${}^{10}\text{Li}$ nuclei produced in the fragmentation reaction ${}^{18}\text{O} + \text{C} \rightarrow n + {}^{10}\text{Li} + X$ at 80 MeV/A in collinear geometry at 0° . The relative-velocity spectrum for $n + {}^9\text{Li}$ was studied. Only a single peak corresponding to low-energy neutrons from ${}^{10}\text{Li}$ was observed. The neutron binding energy in ${}^{10}\text{Li}$ is lower than in Ref. 12. However, the observed peak could also be associated with an excited state

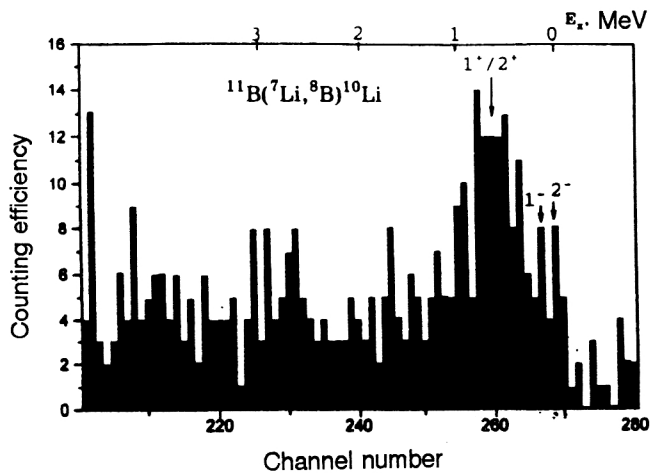


FIG. 6. Spectrum of ^8B nuclei from the reaction $^{11}\text{B}(^7\text{Li}, ^8\text{B})^{10}\text{Li}$ at energy 130 MeV and angle 5° in the lab frame. The ^{10}Li excitation energy is shown on the upper scale. The high energy resolution (70 keV) made it possible to resolve the ground 2^- and first excited 1^- levels of the ^{10}Li nucleus and to distinguish them from the $1^+/2^+$ doublet.

of ^{10}Li decaying with a transition to the first excited state of ^9Li .

Measurements made in Germany¹⁶ found a ^{10}Li mass excess of $33.445(50)$ MeV. Two different reactions were used: $^9\text{Be}(^{13}\text{C}, ^{12}\text{N})^{10}\text{Li}$ with $E_{\text{lab}}=336$ MeV (Fig. 7) and $^{13}\text{C}(^{14}\text{C}, ^{17}\text{F})^{10}\text{Li}$ with $E_{\text{lab}}=337$ MeV (Fig. 8). According to the data of this study, the ^{10}Li nucleus is neutron-unstable with neutron binding energy $-0.42(5)$ MeV. In the analysis of the first reaction a low-lying excited state was found at $0.38(8)$ MeV. This state and the ground state may, in the opinion of the authors of that study, with high probability be identified as a $1^+/2^+$ doublet with configuration $[\pi 1p_{3/2} \otimes \nu 1p_{1/2}]$. Here the ground state has $J^\pi=1^+$. The reaction $(^{13}\text{C}, ^{12}\text{N})$ populates the 1^+ state, which is induced by spin-isospin flip in the leading part of the transition amplitude. The 2^+ state corresponds to the mass given in Ref. 8

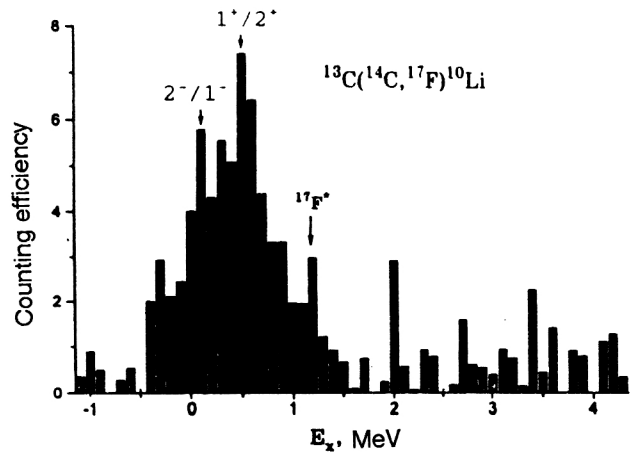


FIG. 8. Spectrum of ^{17}F nuclei from the reaction $^{13}\text{C}(^{14}\text{C}, ^{17}\text{F})^{10}\text{Li}$ at energy 337 MeV and angle 5.4° in the lab frame.⁵⁸ The locations that we propose for the centroids of the 2^- , 1^- and 1^+ , 2^+ level doublets are shown. The energy resolution does not allow the levels of the doublets to be resolved.

for the ground state of ^{10}Li . The second excited state is observed at $4.05(10)$ MeV with width $0.7(2)$ MeV and can have the configuration $\nu 1d_{5/2}$. The data on the second reaction fully support the doublet ground-state interpretation (Fig. 8). The excited state at 4.05 MeV is not observed in this reaction.

(3) Indirect data on the unstable ^{10}Li nucleus have been obtained in studies of the neighboring stable and unstable nuclei ^9Li , ^{11}Li , ^9He , ^{11}Be , and so on.⁷ Regarding the ^9Li nucleus, it is known⁷ that it is particle-stable and has spin and parity $J^\pi=\frac{3}{2}^-$, isospin $T=3/2$, and radius 2.41 F. The ^9He nucleus⁷ is particle-unstable. The transverse-momentum distribution has a maximum at zero and falls with increasing P_\perp (Ref. 22). The mass excess is 40.80 ± 0.10 MeV. The ^9He nucleus decays into the channel $^8\text{He}+n$ with energy 1.13 MeV. The ground state has characteristics $J^\pi=\frac{1}{2}^-$ according to the shell-model calculations.¹⁰ The ^{11}Li nucleus²³ is particle-stable, and its mass excess is 40.85 ± 0.08 MeV. The two-neutron separation energy is 247 ± 80 keV. The nuclear spin is $3/2$, and the systematics indicate negative parity. The nuclear radius is anomalously large: 3.16 ± 0.11 F. This is apparently related to the neutron halo.²⁴ The ^{11}Be nucleus is particle-stable,²³ and it has spin $1/2$, anomalous positive parity, $T=3/2$, and anomalously large nuclear radius: 2.86 ± 0.04 F, which is due to the neutron halo.^{24,25} The ^{12}B nucleus is particle-stable and has $J^\pi=1^+$ and $T=1$ (Ref. 23).

2. METHODS OF THEORETICAL ANALYSIS

There are several well known model and model-independent approaches to the theoretical analysis of the experimental data, in addition to semiempirical mass formulas and extrapolation rules following from the systematics of nuclear properties. When extrapolating the properties of stable and particle-stable nuclei to the region of exotic particle-unstable nuclei it is usually necessary to make use of all the techniques available. They complement each other and make it possible to predict the characteristics of unknown nuclei with a high degree of reliability. Let us review the basic techniques which are widely used at present.

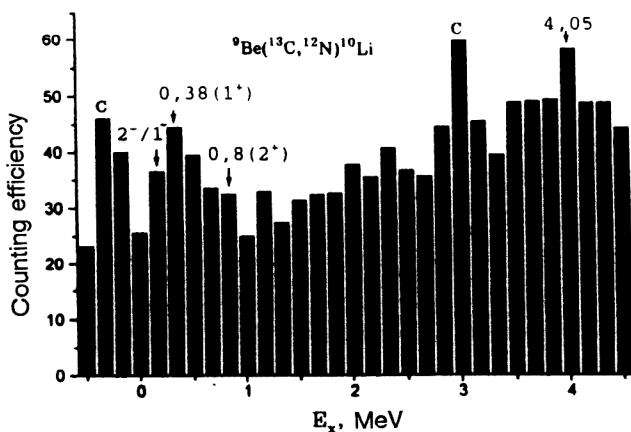


FIG. 7. Spectrum of ^{12}N nuclei from the reaction $^9\text{Be}(^{13}\text{C}, ^{12}\text{N})^{10}\text{Li}$ at energy 336 MeV and angle 3.8° in the lab frame near the ^{10}Li ground state. The carbon lines (C) and the location of the 2^- , 1^- doublet proposed here are shown. The indicated locations of the 1^+ , 2^+ levels and the level at 4.05 MeV correspond to the data of Refs. 58 and 59.

2.1. Shell-model calculations

In the current version of the shell model^{10,26} the Hamiltonian is split into two parts, one of which depends on the coordinates of the nuclear center of mass, and the other on the relative coordinates of the two nucleons i, j :

$$H = \sum_{i=1}^A \left(P_i^2/2m + \frac{1}{2}m\omega^2 r_i^2 \right) + \sum_{i < j} [V_{ij} - (m\omega^2/2A)(r_i - r_j)^2],$$

where P_i is the momentum, m is the mass, r_i is the nucleon coordinate, and ω is the oscillator frequency.

For a potential V_{ij} depending only on the relative coordinates the Hamiltonian is translationally invariant, and the unphysical states associated with excitation of the center of mass can be eliminated by the method of Ref. 27. The Hamiltonian does not reflect the individual properties of nuclei. Therefore, model calculations of the nuclear levels can only lead to qualitative agreement with the experimental data. Coulomb corrections have been introduced to improve the description of the data.^{11,26} When they are included, the errors in determining the level energies can be reduced from ≈ 1 MeV to 0.3–0.5 MeV for stable light nuclei in the region $N \approx Z$. The authors of Ref. 10 attempted to describe the binding energies of exotic neutron-rich light p -shell nuclei together with the spins and parities of their four lowest states. In particular, for the two lowest states of ^{10}Li the two versions of the calculation using $(0+1)\hbar\omega$ and $(0+2)\hbar\omega$ model spaces gave positive parities with level ordering 1^+ , 2^+ and 2^+ , 1^+ , respectively. The distance between them is 0.65 MeV. The neutron binding energy ε_n is -0.61 and -0.65 MeV, respectively, for these two models. These results cannot be very reliable, because the average discrepancy between theory and experiment is acknowledged by the authors of Ref. 10 to be 1.1 and 1.2 MeV, respectively, for these models. The results obtained in the shell-model calculations of Ref. 26 are considerably more reliable. Here the prediction that the ground state of ^{10}Li has spin and parity 2^- is based on calculations of the lowest $T=2$ state of the stable ^{10}B nucleus. The shell-model calculations are apparently better in the region $N=Z$. We think that for nuclei far from the region $N=Z$ it is necessary to introduce into the Hamiltonian a dependence on the number of excess (or deficient) nucleons in the nucleus.

2.2. The isobaric-multiplet mass equation (Ref. 28)

When the nuclear forces are assumed to be charge-independent, all the members of an isospin multiplet T have the same energy. The isobaric symmetry is broken by the electromagnetic interaction. Additional effects arise from the difference between the neutron and proton masses.⁶ The lifting of the energy degeneracy of the $(2T+1)$ members of the isospin multiplet is described by the mass equation of the isobaric multiplet²⁹ describing the dependence of the mass on the third projection T_z of the isospin T :

$$M(A, T, T_z) = a(A, T) + b(A, T)T_z + c(A, T)T_z^2. \quad (1)$$

The coefficient a includes (among other things) the average Coulomb energy of the multiplet. The coefficient b depends linearly³⁰ on $A^{2/3}$:

$$b(\text{keV}) = (-733.5 \pm 0.7)A^{2/3} + (1771.0 \pm 0.1). \quad (2)$$

Comparison of the experimental ratio b/c with the model of Ref. 31, assuming that the nucleus is a uniform sphere of constant charge density, leads to a linear dependence on A for $T=3/2$ and 2 (Ref. 28):

$$-\frac{b}{c} = \alpha A - \beta; \quad \alpha = 0.97; \quad \beta = 4.33. \quad (3)$$

The theoretical curve³¹ is shifted upwards relative to the experimental curve by $\Delta\beta=0.33$, while the correct slope α is preserved.

The Coulomb rearrangement energy ΔE_c for the analog levels of two neighboring nuclei is defined as

$$\Delta E_c(A, T, T_z - 1 | T_z) = M_{Z>} - M_{Z<} + \Delta_{nH}, \quad (4)$$

where $M_{Z>}$ is the mass of the member of highest order in Z , $M_{Z<}$ is the mass of the member of lowest order in Z , and $\Delta_{nH}=0.782339(17)$ MeV is the difference between the neutron and hydrogen-atom masses. The parameters b and c are related to ΔE_c as³⁰

$$\Delta_{nH} - b(A, T) = (T - 1/2)\Delta E_c(A, T, T - 2 | T - 1) - (T - 3/2)\Delta E_c(A, T, T - 1 | T); \quad (5)$$

$$c(A, T)/3 = 1/6[\Delta E_c(A, T, T - 2 | T - 1) - \Delta E_c(A, T, T - 1 | T)]. \quad (6)$$

The mass equation (1) can be used to determine the energies of the states of all the members of the isobaric multiplet with given values of A and T up to several tens of keV if the energy of at least one member of this multiplet is known for determining the coefficient a . The mass equation sometimes includes terms with higher powers of T_z (Ref. 32), $dT_z^3 + eT_z^4$. In second-order perturbation theory these include nondiagonal matrix elements. However, the errors in the determination of the coefficients d and e are large, often larger than the coefficients themselves. These terms have not been included in our calculations.

2.3. The theory of threshold phenomena

This theory is applicable to the study of nuclear states near the reaction threshold (Refs. 19, 33, and 34). The possibility of such study is based on the analytic energy dependence of the wave function, which is well known for $kR \ll 1$, and for charged particles also for $\eta \gg 1$ (Refs. 35–37), where k is the wave number, R is the nuclear radius, and η is the Coulomb parameter. The use of only a small number of partial waves at low energies makes it possible to represent the wave function as an analytic function of energy with a limited number of parameters. This function is then used to approximate the experimental data in the analysis of threshold phenomena,¹⁹ and the parameters containing physical information about the reaction mechanism and the properties of the compound nucleus are found. In particular, the energy of the state of the compound nucleus, the total and partial

widths of this state, and also its parity (orbital angular momentum l) are found. This information makes it possible to determine the type of threshold state and its isospin for the purpose of extrapolating the results of the analysis to neighboring members of the isobaric multiplet^{17,18} by using the mass equation (1). The advantage of the theory of threshold phenomena is that the number of parameters is small, ≈ 10 . The accuracy of the calculations is determined by the experimental errors and is practically independent of the version of the theory that is used.

2.4. Model-based methods of analysis

The threshold analysis is also carried out³⁸ by means of R -matrix theory³⁹ with expansion of the penetration factor $P_l(E)$ in powers of the energy. However, the complicated nature of the coupling between the R matrix and the collision matrix makes the R -matrix approach ineffective: there are too many parameters (≈ 100), many of which have no physical meaning.⁴⁰ The result of the analysis depends on the version of the theory that is used.

The resonating-group method is more effective. Owing to the complexity of the calculations, it is applicable to light nuclear systems with no more than three clusters in the nucleus.^{41,42} Representation of the wave function of the system as a series in the multiparticle basis of oscillator functions makes it possible to reduce the many-body problem to the solution of a system of linear algebraic equations:

$$\sum_{\nu', \alpha'} \langle \alpha, \nu | H - E | \nu', \alpha' \rangle C_{\nu'}^{\alpha'} = 0, \quad (7)$$

where H is the Hamiltonian and $|\nu, \alpha\rangle$ are basis functions. The relative simplicity of these equations compared with the multidimensional Schrödinger or Faddeev–Yakubovskii equations⁴³ makes this method attractive for analyzing nuclear reactions, including near-threshold ones. The infinite system of equations (7) must be truncated in a manner depending on the sophistication of the computational technique. Some part of the complete basis is chosen according to the model representations of the physics of phenomena in this system. The effect of the rest of the basis not used in the solution is taken into account by the introduction of certain free parameters. One of them is the oscillator frequency, which is chosen so as to obtain the best description of the structural features of the system. Two-particle realistic potentials with parameters describing the interaction of two free nucleons are used as the nucleon–nucleon interaction potentials. Sometimes these parameters vary significantly (by up to 20%). The Volkov⁴⁴ and Hasegawa–Nagata⁴⁵ realistic potentials are the ones used most often.

Naturally, the results of the calculations using the resonating-group method depend significantly on the choice of basis functions and on the parameters of the realistic potentials. For the calculations to have predictive power it is necessary to select all the parameters so as to obtain the best description of the available experimental data.

The method of harmonic polynomials (the K -harmonics method; Ref. 46) has been used rather successfully to describe the ground and lowest excited states of nuclei, includ-

ing exotic nuclei.⁴⁷ This method takes its name from the expansion of the wave function of the system in a series in eigenfunctions $U_{k\gamma}$ of the angular part of the multidimensional Laplacian Δ :

$$\Delta_\Omega U_{k\gamma} = -K(K+3A-5)U_{k\gamma},$$

where $K \geq K_{\min}$ are positive integers, γ is the set of all the other quantum numbers, and Ω is the set of angular variables. The radial functions $X_{k\gamma}(\rho)$ depend on the collective variable ρ :

$$\rho^2 = \sum_{i=1}^A (\mathbf{r}_i - \mathbf{R})^2$$

and satisfy a system of second-order ordinary differential equations. The spectrum of nuclear levels with K_{\min} approximated by using the techniques developed in the shell model⁴⁸ can be represented in terms of harmonics with given values of the total angular momentum J and isospin T , as in the shell model. However, only some of the levels following from the equations for the K harmonics are obtained in the shell approach. The spectrum from the K harmonics is richer, because it contains excitation of collective motion in the variable ρ , which generates entire bands of states.

In this sense the nuclear spectrum in the resonating-group method is even richer in collective states, because it contains a larger number of collective degrees of freedom corresponding to the internal motion of different clusters. The question of the type of two-nucleon potential in the K -harmonics method is not a simple one because the saturation conditions must be satisfied. Potentials in the form of a superposition of Gaussian potentials, one of which is repulsive, are usually used.⁴⁹ Here the potential parameters are fitted so as to obtain the best description of the nucleon–nucleon scattering phase shifts in a fairly wide energy range. Soft-core one-boson exchange potentials and velocity-dependent potentials like the Bryan–Scott potential⁵⁰ are attracting a great deal of attention. As the number of nucleons in the nucleus increases the system becomes more and more unstable to collapse. The calculations of the properties of $1s$ -shell nuclei are very accurate. A great deal of effort is required to obtain good accuracy for $1p$ -shell nuclei. The so-called P model⁵¹ or the method of angular potential functions⁵² has been proposed for them. In this method the wave function of the system is represented as a sum of terms, where the leading one is the wave function Ψ_0 of the K -harmonics method in the K_{\min} approximation, while the other terms are supposed to be small corrections to the leading one. The role of the corrections reduces to the replacement of the matrix elements of the nucleon–nucleon interaction by the effective matrix elements in the system of differential equations for the radial wave functions in the corrections to the leading Ψ_0 term. The angular potential functions entering into the correction terms are constructed by using the technique of j -raising operators (in the jj coupling scheme) from K_{\min} harmonics with given quantum numbers J^π and T .

A realistic soft-core potential is chosen as the nucleon–nucleon interaction.⁵³ Accordingly, in the P model⁵¹ the wave function includes not only harmonics with K_{\min} and certain J

and T , but also terms of higher order in K in agreement with the radial equations. On the basis of general considerations this must lead to a better description of the characteristics of light nuclei than in the shell model and in the K -harmonics method. Calculations have shown that the binding energies of the ${}^6\text{Li}$ nucleus and $1s$ -shell nuclei are described better in the P model. In the method of angular potential functions,⁵² after the radial equations are written down they are treated as auxiliary conditions on the matrix elements of the nucleon–nucleon (NN) potentials for the purpose of solving the inverse problem: reconstructing the matrix elements of the NN potentials. The matrix elements reconstructed by using the experimental data are then again substituted into the radial equations. The process of alternate solution of the direct and inverse problems is repeated several times until the required accuracy is obtained or until the reconstructed potential satisfies the Calogero–Simonov saturation conditions.⁵⁴ The correction of the potential eliminates the “overbinding” of ≈ 10 MeV of heavy p -shell nuclei (${}^{16,15}\text{O}$), after which analysis of the isotopes ${}^{10,9}\text{He}$ becomes reasonable. For them, complete convergence of the expansion of the wave function in the potential-harmonics series is obtained when ≈ 200 basis functions are included in the space of multidimensional angles. According to the calculation, the isotopes ${}^9\text{He}$ and ${}^{10}\text{He}$ are nuclear-unstable. The heavy isotopes ${}^{7,8,9}\text{H}$ are far from being bound states, and there are no resonance states of these systems. The ground state of ${}^6\text{H}$ has high energy $\varepsilon = 6.3$ MeV relative to the threshold for the breakup ${}^6\text{H} \rightarrow {}^3\text{H} + 3n$.

There is no clearly manifested quasistationary state in the ${}^5\text{H}$ system. However, in the opinion of the authors of Ref. 52, the results are not unambiguous. In our opinion, the methods for calculating nuclear spectra developed in Refs. 51 and 52 represent mathematical schemes for solving multidimensional Schrödinger equations with a truncated K -harmonics basis (or a shell-model basis). In these schemes the infinite part of the basis is replaced by another finite basis, and the matrix elements of the NN potential in the radial equations are replaced by certain effective matrix elements. A prescription is given for the alternate optimization of the restricted auxiliary basis and the effective matrix elements, using the available experimental data. In some cases these schemes may permit the characteristics of nuclei to be described more accurately than in the K -harmonics method and in the shell model, but this is achieved at the cost of losing the completeness of the physical picture. Here the NN potential loses universality and acquires individual properties characterizing the nucleus for which it is optimized. Moreover, the NN potential will depend on the completeness of the experimental data for a given nucleus and on the specific choice of the data used in the optimization. Owing to these considerations, we should take particular care when dealing with the results of Refs. 51 and 52.

The K -harmonics method in the three-body approximation ${}^9\text{Li} + n + n$ has found an interesting application in calculations of the characteristics of the exotic nucleus ${}^{11}\text{Li}$ (Ref. 47). The interaction potentials for cluster pairs are chosen to have Gaussian form.⁵³ The wave function is written as a series in hyperspherical harmonics depending on the principal quantum number K up to $K = 12$. All the orbital angular

momenta are assumed to be zero, as in Ref. 53. The calculations of the binding energy (0.3 MeV), the matter radius (3.32 F), and the momentum distribution are in satisfactory agreement with experiment. The distance between the center of mass of ${}^9\text{Li}$ and an external neutron is 6.4 F. It follows from the calculation that the S -wave potential in the ${}^9\text{Li} + n$ subsystem is attractive.

Results similar to those of Ref. 47 have been obtained in Ref. 53 by a variational three-body calculation for ${}^9\text{Li} + 2n$. The potentials were chosen in the form of a sum of several Gaussians. The ground-state wave function is written in terms of the harmonic-oscillator wave functions. The calculations give ${}^{10}\text{Li}$ unbound by 0.29 MeV. The wave function is 99% saturated by the $l=0$ harmonic. Therefore, the version with negative parity of the ${}^{10}\text{Li}$ nucleus is actually supported in Refs. 47 and 53.

It is interesting to try to calculate the ground state of ${}^{10}\text{Li}$ in the RPA model,^{58,59} which is applicable to intermediate and heavy nuclei. The calculations revealed a strong $\frac{1}{2}^-$ neutron resonance in the ${}^9\text{Li} + n$ system at energy 0.26 MeV with a narrow width $\Gamma = 0.05$ MeV. Therefore, according to the calculations, the ground state of ${}^{10}\text{Li}$ has positive parity [$J^\pi({}^9\text{Li}) = \frac{3}{2}^+$].

With this we conclude our review of the experimental and theoretical studies devoted to ${}^{10}\text{Li}$. They have given a large amount of information, which often differs and is even contradictory. A guiding thread is needed to analyze it and evaluate it correctly. For this we shall use our recent results from analysis of the excitation function of the reaction ${}^7\text{Li}(t, p){}^9\text{Li}$ near the neutron threshold of the reaction ${}^7\text{Li}(t, n){}^9\text{Be}^*$ ($E_x = 14.3922$ MeV, $J^\pi = \frac{3}{2}^-$, $T = 3/2$). These results can be used as a reference, since their reliability is high ($>90\%$) and they are based on experimental data with an error of less than 0.5%.

3. THEORETICAL ANALYSIS OF THE EXCITATION FUNCTION OF THE REACTION ${}^7\text{Li}(t, p){}^9\text{Li}$ NEAR THRESHOLD

3.1. Relations from the theory of threshold phenomena

The experimental results described in the preceding section on the integrated cross section of the reaction ${}^7\text{Li}(t, p){}^9\text{Li}$, which were obtained by continuous measurement,⁵ possess high accuracy ($\approx 0.5\%$) and stability, i.e., small spread. These results have served as the basis for theoretical analysis. They contain 99 experimental points near the threshold of the reaction ${}^7\text{Li}(t, p){}^9\text{Be}(J^\pi = \frac{3}{2}^-, T = 3/2, E_x = 14.3922 \text{ MeV})$.

The theory of threshold phenomena, described in the review of Ref. 19, was used for the analysis. In this theory the squared absolute value of the collision matrix is written as

$$|U_{ps'l'ts}^{J\pi}|^2 = |Z_{pl't}|^2 |M_{ps'l'ts}^{J\pi}|^2 |Z_{tl}|^2, \quad (8)$$

where the matrix Z characterizes the penetrability of the Coulomb and centrifugal barriers, M is the reduced collision matrix, s is the channel spin, J is the total angular momentum, π is the parity, l is the orbital angular momentum, and p

and t are the other quantum characteristics of the exit and entrance channels, respectively. Near the zero of energy ($kD \ll 1$, $\eta \gg 1$),

$$|Z_l| = \frac{2\pi\eta}{e^{2\pi\eta}-1} \frac{(kD)^{2l+1}}{[(2l-1)!!]^2} \prod_{m=1}^l \left(1 + \frac{\eta^2}{m^2}\right) = \frac{\pi}{e^{2\pi\eta}-1} X_l; \quad (9)$$

$$D = \frac{1}{2k\eta}; \quad \eta = \frac{z_1 z_2 e^2 \mu}{\hbar^2 k};$$

$$X_l = \frac{(kD)^{2l}}{[(2l-1)!!]^2} \prod_{m=1}^l \left(1 + \frac{\eta^2}{m^2}\right),$$

where z_1 and z_2 are the nuclear charges, μ is the reduced mass, k is the wave number of the relative motion, and l is the orbital angular momentum.

For $kD \gg 1$ the matrix Z depends weakly on energy and can be set equal to a positive real quantity, say, unity:

$$|Z_l| = \text{const} = 1. \quad (10)$$

The square of the reduced collision matrix for the transition from a threshold to a nonthreshold channel near the neutron threshold channel is

$$|M_{t,p}^{J\pi}|^2 = |\mathcal{M}_{t,p}^{J\pi}|^2 \{1 - \theta(E_n) |Z_{t,n}| |\mathcal{M}_{t,n}^{J\pi}|^2\}, \quad (11)$$

where

$$Z_{t,n} = \frac{(k_n D_n)^{2l_n+1}}{[(2l_n-1)!!]^2}; \quad \theta(E_n) = \begin{cases} 1, & E_n > E_q \\ 0, & E_n < E_q \end{cases}.$$

Here D_n is a quantity of the order of the radius of the ^9Be nucleus. The matrix \mathcal{M} is defined as

$$\mathcal{M}_{ij}^{J\pi} = 2 \left(m_{ij}^{J\pi} + \sum_N \frac{(a_{ij}^{J\pi})_N}{E - E_N^{J\pi} + i\Gamma_N^{J\pi}/2} \right); \quad ij = i, j = t, p, n, \quad (12)$$

where N_0 is the number of resonance states with given values of J and π .

When there is a single resonance state for a given set of quantum numbers J , π , the summation over N is removed. For conciseness of notation, sets of channel quantum numbers will sometimes be replaced by $i, j = ij$. If the state in question does not have a resonance, the reduced amplitude id $a_{ij}^{J\pi} = 0$. In the case $N_0 = 1$,

$$|a_{ij}^{J\pi}| = \gamma_i^{J\pi} \gamma_j^{J\pi}, \quad (13)$$

where γ_k is the partial amplitude of the reduced decay width. It is related to the observed partial decay width as

$$\Gamma_k = 2|Z_k| \gamma_k^2, \quad (14)$$

and the total width is

$$\Gamma = \sum_k \Gamma_k. \quad (15)$$

On the scale of excitation energy of the compound nucleus ^{10}Be the threshold of the proton channel

$E_{qp} = 19.636$ MeV is separated from the threshold of the neutron channel $E_{qn} = 21.205$ MeV by 1.569 MeV in the c.m. frame.⁷ We shall restrict the number of partial waves in the proton channel to three values $l \leq 2$. The triton threshold $E_{qt} = 17.251$ MeV lies 3.954 MeV from the neutron threshold, which is a distance large enough that the energy dependence of Z_{tl} can be neglected and we can set $|Z_{tl}| = 1$ (10).

As a result of these restrictions the integrated cross section for the reaction $^7\text{Li}(t, p)^9\text{Li}$ can be written as

$$\sigma_{p,t} = \frac{4\pi^2 g}{8k_t^2 (e^{2\pi\eta_p}-1)} \left\{ X_0 (3|M_{p10,t10}^{1-}|^2 + 5|M_{p20,t20}^{2-}|^2) + X_1 \sum_{J=0}^3 \sum_{ss'} (2J+1) |M_{ps't,tsl}^{J+}|^2 + X_2 \sum_{J=0}^4 \sum_{ss'l} (2J+1) |M_{ps'2ltsl}^{J-}|^2 \right\}, \quad (16)$$

where $X_0 = 1$, $X_1 = (kD)^2 + \frac{1}{4}$, $X_2 = X_1[(kD)^2 + \frac{1}{16}]/9$, $g = 1/8$, and the wave number k_t and η_p are given in the lab frame of the incident tritons. The cross section (16) was used as the approximating function for describing the experimental excitation function given in Ref. 5 and in Fig. 2. The adjustable parameters were

$$|m_{ij}|, |a_{ij}|, \arccos \frac{(ma)_{ij}}{m_{ij} a_{ij}}, E^{J\pi}, \Gamma^{J\pi}$$

and the coefficients of the various powers of the energy. The total number of parameters varied from 19 (for the s -neutron threshold) to 21 (for the p -neutron threshold).

3.2. Numerical analysis of the excitation function

The goal of the analysis of the experimental data is to answer two questions: (1) how many levels of the compound nucleus ^{10}Be are located in the threshold region under consideration, $E_t = 5.4-5.95$ MeV; (2) what are the quantum characteristics and, in particular, the parities of these levels. The answers can be obtained by analyzing the experimental data by using the least-squares method with the approximating function (16) with one or two resonance matrix elements $M^{J\pi}$ with all possible combinations of parities.

Assuming that ^{10}Be has two levels near threshold, we analyzed three possible situations:

- (1) $\pi_1 = \pi_2 = -$; (2) $\pi_1 = -, \pi_2 = +$,
- (3) $\pi_1 = \pi_2 = +$. (17)

In the cases with identical parities we did not analyze the situations with $J_1 = J_2$, where effects of two-resonance interference should be seen according to Eq. (12). Interference has not been observed experimentally.

The results of the analysis of the three situations (17) are given in Table I.

The analysis demonstrates the following: (1) one resonance always lies to the left of the neutron threshold $E_{qn} = 5.649$ MeV, and the second lies to the right, independently of the parity of the resonances; (2) a resonance with

TABLE I. Characteristics of two levels of the compound nucleus ^{10}Be in the energy range $E_i=5.4-5.95$ MeV in the lab frame. Here $E^{(j)}$ and $\Gamma^{(j)}$ are the resonance energies and widths for states with angular momentum $j=1, 2$. All energies are in MeV.

π_1, π_2	Number of parameters	χ^2	$E^{(1)}$	$\Gamma^{(1)}$	$E^{(2)}$	$\Gamma^{(2)}$	$\sqrt{2J_1+1}a_{p,t}^{(1)}$	$a_{n,t}^{(1)}$	$\sqrt{2J_2+1}a_{p,t}^{(2)}$	$a_{n,t}^{(2)}$
- -	19	127.5	5.595	0.114	5.687	0.086	0.019	0.020	0.023	0.059
+ -	21	238.3	5.326	1.220	5.651	0.083	0.810	0.100	0.023	0.169
+ +	21	337.9	5.250	1.578	5.695	0.080	1.099	0.034	0.011	0.291

negative parity, if it exists, always lies above threshold; (3) the location of the second resonance in all cases differs insignificantly, namely, within 40 keV, which can be attributed to the target thickness of more than 20 keV and the error in determining the resonance energy; (4) the widths of the second resonance practically coincide. Regarding the resonance below threshold, it can be stated that the characteristics for different parities differ fundamentally. To check the agreement of the three theoretical hypotheses with the empirical data we used the F criterion:⁵⁵

$$F_{21} = \frac{\chi^2(f_2)}{f_2} \bigg/ \frac{\chi^2(f_1)}{f_1} = 1.87;$$

$$F_{31} = \frac{\chi^2(f_3)}{f_3} \bigg/ \frac{\chi^2(f_1)}{f_1} = 2.66. \quad (18)$$

Here f is the number of degrees of freedom of the χ^2 distribution. From the table of quantiles of the F distribution⁵⁵ we find that variants 2 and 3 in (17) can be rejected with a probability of more than 99%.

Let us now assume that in the energy range in question, $E_i=5.4-5.95$ MeV, the ^{10}Be nucleus has one level. Let us try to determine its parity by comparing two hypotheses: (1) the level has negative parity, (2) the level has positive parity. The approximation of the experimental data⁵ by the function (16) with a single resonance matrix element of the corresponding parity by means of the least-squares method gives the results shown in the first two rows of Table II. Comparison using the F criterion gives $F_{21}=1.6$. This result implies that the hypothesis of negative parity in the one-level description is correct with greater than 95% probability.

Let us now compare the most probable hypotheses in the two- and one-level descriptions in order to answer the question of how many levels does the ^{10}Be nucleus have in the energy range $E_i=5.4-5.95$ MeV. From the first rows of Tables I and II we find $F_{21}=2.62$. From the tables of quan-

tiles it follows that there are two levels with a probability of greater than 99%. The parities of these two levels were determined earlier: they are negative.

Thus, analysis of the experimental data has provided the answers to two questions. How should we deal with the later data²⁰ obtained in the pulsed operating mode? The approximation of these data by the function (16) in the one-level description gave the results in the third and fourth rows of Table II. It is clearly seen that the results of the approximation of the experimental data in Refs. 20 and 5 are close enough. However, an attempt to describe the data of Ref. 20 in the two-level variant was unsuccessful, owing to the point spread below the neutron threshold. In what follows we shall view the existence near the neutron threshold of two levels with negative parities and parameters given in the first row of Table I as an established fact. In addition, in the numerical analysis of this variant we obtained the following relations for the reduced nonresonance amplitudes:

$$\sqrt{2J_1+1}|m_{pt}^{(J_1)}| = 0.0662; \quad \sqrt{2J_2+1}|m_{pt}^{(J_2)}| = 1.19;$$

$$l=0, s=J. \quad (19)$$

These can be used to try to estimate the total angular momenta J_1 and J_2 , although it is impossible to determine them rigorously from the integrated cross section. Since the spins of the ^7Li and ^9Li nuclei in the ground state and also of the $^9\text{Be}^*$ nucleus produced in the neutron threshold channel are $3/2$ while the parities are negative, in all three channels the total angular momentum for $l=0$ takes two values: $J=1, 2$.

Owing to the large number of open channels with different quantum characteristics, it can be expected that two non-resonance states of the same type in the same channel give comparable contributions. We do not consider the data to be sufficient for determining the contribution of any other channels except the p channel, in order to be able to use the unitarity relation satisfied by the collision matrix. From the condition that the amplitudes (19) be comparable we find

$$J_1=1, \quad J_2=2. \quad (20)$$

Therefore, to the ^{10}Be level lying below threshold we assign angular momentum 1, while to the level above threshold we assign angular momentum 2. We shall use this estimate in what follows, although it is not reliable. However, it does not significantly affect our further calculations and conclusions.

Let us find the ratio of the reduced neutron and proton partial widths from the resonance amplitudes in Table I:

TABLE II. Parameters of one resonance of ^{10}Be near threshold. All energies are in MeV in the lab frame.

N	Number of experimental points	Level parity	χ^2	Number of parameters	$E^{(1)}$	$\Gamma^{(1)}$
1	99[5]	(-)	332.6	13	5.725	0.146
2	99[5]	(+)	526.9	15	5.538	0.094
3	135[20]	(-)	1382	13	5.685	0.146
4	135[20]	(+)	1818	15	5.715	0.117

TABLE III. Characteristics of the spin doublet of ^{10}Be levels near the threshold $E_q = 21.205$ MeV of the decay $^{10}\text{Be} \rightarrow n + ^9\text{Be}$ ($J^\pi = \frac{3}{2}^-$, $T = 3/2$, $E_x = 14.3922$ MeV).

E_x , MeV	J^π, T	Γ , keV	$(\gamma_n'/\gamma_p')^2$
21.168 ± 0.050	$(1)^-, 2$	80 ± 45	$3.324 (5.540)$
21.232 ± 0.018	$(2)^-, 2$	60 ± 40	$32.902 (19.741)$

$$\left(\frac{\gamma_n^{1-}}{\gamma_p^{1-}}\right)^2 = 3.324(5.540);$$

$$\left(\frac{\gamma_n^{2-}}{\gamma_p^{1-}}\right)^2 = 32.902(19.741). \quad (21)$$

In the parentheses we give the results for the case which is the opposite of (20), i.e., when the subthreshold level has angular momentum 2 and the above-threshold level has angular momentum 1. In crossing the threshold we see strong growth of the neutron mode of motion (in both cases). Let us summarize our results on the near-threshold levels of ^{10}Be . Both levels have widths less than 100 keV in the c.m. frame, and on the basis of this we can assign isospin $T=2$ to them. The characteristics of these levels are given in Table III. For estimating the partial widths we can assume that $\gamma_i' = \gamma_p'$, which is very probable, owing to the large separation of the thresholds of the t and p channels from the neutron threshold. Then from Table I we find

$$(\gamma_i')^2 \approx (\gamma_p')^2 \approx 10 \text{ keV}, \quad (\gamma_n^{2-})^2 = 336 \text{ keV},$$

$$(\gamma_n^{1-})^2 \approx 38 \text{ keV},$$

$$\Gamma_i' \approx 20 \text{ keV}, \quad \Gamma_p' \approx 8 \text{ keV},$$

$$\Gamma_n^{2-} \approx 28 \text{ keV}, \quad \Gamma_n^{1-} = 0. \quad (22)$$

It follows from these partial widths that all modes of motion are collective, except for the neutron mode in the above-threshold 2^- level, where the partial width $(\gamma_n^{2-})^2$ is close to the one-particle width. This state of the ^{10}Be nucleus is the $^9\text{Be}^*$ core ($E_x = 14.3922$ MeV) and a weakly bound neutron.

Both levels in the shell-model theory are the $1s^4 1p^5 2s$ configuration with interrupted filling sequence.

4. ANALOG PREDICTION OF THE PROPERTIES OF LEVELS OF ^{10}Li

The levels of the ^{10}Be nucleus found from the experimental data⁵ are the lowest states with $T=2$, i.e., they are the analogs of the ground and first excited states of ^{10}Li (and also ^{10}N). We shall use the isobaric-multiplet mass equations (IMMEs) and the systematics of the Coulomb rearrangement energies²⁸ to extrapolate the characteristics of $T=2$ levels of the well known ^{10}B and ^{10}Be nuclei to the little studied ^{10}Li , ^{10}C , and ^{10}N nuclei. The mass equation is (1). The coefficient a includes the average Coulomb energy for the given isobaric multiplet. It is equal to the mass excess of ^{10}B plus the excitation energy of the first level with $T=2$. According to Ref. 56,

$$a(A=10, T=2) = [12.051 + (23.1 \pm 0.1)] \text{ MeV}$$

$$= (35.151 \pm 0.1) \text{ MeV}. \quad (23)$$

The coefficient b was obtained in Ref. 28 by a fit to the experimental data:

$$b(A, T) = (-0.7335A^{2/3} + 1.771) \text{ MeV}$$

$$= -1.6336 \text{ MeV}. \quad (24)$$

The coefficient c was determined from the linear dependence of the ratio $-b/c$ on A for $T=3/2$ and 2:

$$-\frac{b}{c} = 0.97A - 4.33; \quad c = 0.304 \text{ MeV}. \quad (25)$$

The mass equation (1) with coefficients (23)–(25) describes the masses of all the members of the multiplet with $A=10$, $T=2$ with an accuracy of at best several tens of keV. To calculate the positions of the levels of the $(1^-, 2^-)$ spin doublet in ^{10}Li it is necessary to find the Coulomb rearrangement energy ΔE_c for pairs of neighboring nuclei $^{10}\text{Be} \rightarrow ^{10}\text{Li}$ and $^9\text{Be} \rightarrow ^9\text{Li}$. For the latter there is an experimental value²⁸ which we shall use:

$$\Delta E_c(A=9, T=3/2, T_z=1/2 | T_z=3/2) = 1.569 \text{ MeV}. \quad (26)$$

For the pair $^{10}\text{Be} \rightarrow ^{10}\text{Li}$ the Coulomb rearrangement energy is determined from the two equations (5) and (6):

$$\Delta E_c(A=10, T=2, T_z=1 | T_z=2) = 1.444 \text{ MeV}. \quad (27)$$

The value of the Coulomb rearrangement energy (27) will be used to extrapolate the subthreshold 1^- level of ^{10}Be , and the value of ΔE_c in (26) will be used to extrapolate the above-threshold 2^- level, since the ^{10}Be nucleus in this case has the structure of an excited $^9\text{Be}^*$ core plus a weakly bound neutron. We shall use Eq. (4) for the extrapolation. The mass defects of ^{10}Be for the 1^- , 2^- spin doublet are

$$J^\pi = 1^-; \quad \Delta M c^2 = (12.607$$

$$+ 21.168) \text{ MeV} = 33.775 \text{ MeV}, \quad (28)$$

$$J^\pi = 2^-; \quad \Delta M c^2 = (12.607$$

$$+ 21.232) \text{ MeV} = 33.839 \text{ MeV}. \quad (29)$$

Substituting these values and the Coulomb rearrangement energies (27) and (26) into Eq. (4), we find the mass excesses of ^{10}Li for this doublet:

$$J^\pi = 1^-; \quad \Delta M(^{10}\text{Li})c^2 = (33.775 - 1.444$$

$$+ 0.782) \text{ MeV} = 33.113 \text{ MeV}, \quad (30)$$

$$J^\pi = 2^-; \quad \Delta M(^{10}\text{Li})c^2 = (33.839 - 1.569$$

$$+ 0.782) \text{ MeV} = 33.052 \text{ MeV}. \quad (31)$$

In ^{10}Li the levels of the spin doublet have changed places: the 2^- level is the ground state of ^{10}Li , and the 1^- level is the first excited state with energy 61 keV. If, as for the 1^- level, we use the value of the Coulomb rearrangement energy (27) to extrapolate the 2^- level, the mass defect will be

$$J^\pi = 2^-; \quad \Delta M(^{10}\text{Li})c^2 = 33.177 \text{ MeV}. \quad (32)$$

The lower (31) and upper (32) limits on ΔM for the location of the 2^- level in ^{10}Li are thereby determined. Since the ^{10}Li

TABLE IV. Characteristics of the ground and first excited states of the ^{10}Li nucleus.

E_x , MeV	J^π , T	$\Gamma=\Gamma_n$, keV	γ_n^2 , keV	$-S_n$, keV
g.s.	$2^-, 2$	68	336	27
0.061	$1^-, 2$	14	40	88

nucleus is neutron-unstable, its ground state is most probably determined by the lower limit. Let us find the neutron separation energy S_n for ^{10}Li by using the equation

$$S_n(A, Z) = (M(A-1, Z) + M_n - M(A, Z))c^2, \quad (33)$$

where $M_n = 1.008665 \text{ amu} = 939.508 \text{ MeV}$ is the neutron mass. The neutron separation energy for ^{10}Li in the ground 2^- and first excited 1^- states is

$$\begin{aligned} J^\pi = 2^-, \quad S_n &= -27 \text{ keV}, \\ J^\pi = 1^-, \quad S_n &= -88 \text{ keV}. \end{aligned} \quad (34)$$

Our calculations of the energies of the lowest levels of ^{10}Li are based on the systematics of the characteristics of states of known light nuclei. The widths of the levels in the $2^-, 1^-$ spin doublet in ^{10}Li can be estimated from the estimates of the reduced partial widths of this doublet in ^{10}Be , assuming that they are purely $T=2$ isospin (22):

$$(\gamma_n^{2-})^2 = 0.336; \quad (\gamma_n^{1-})^2 = 0.040.$$

Since the decay of ^{10}Li from the two lowest levels occurs via a single neutron channel, the total width of these levels is equal to the neutron width:

$$\Gamma^J = \Gamma_n^J = 2|Z_n|(\gamma_n^J)^2,$$

where $|Z_n| = k_n R$ and R is the ^{10}Li radius. Let us estimate the ^{10}Li radius from the parameters b and c , assuming a uniformly charged sphere:²⁸

$$R(b) = \frac{0.6(A-1)q^2}{\Delta_{nH} - b} = 3.2 \text{ F},$$

$$R(c) = \frac{0.6q^2}{c} = 2.84 \text{ F},$$

where q is the electron charge.

For $R = 3 \text{ F}$,

$$\Gamma_n^{2-} = 68.5 \text{ keV}, \quad \Gamma_n^{1-} = 14.5 \text{ keV}.$$

The calculated characteristics of the ^{10}Li levels are listed in Table IV.

5. COMPARISON OF THE PROPERTIES OF THE PREDICTED LEVELS OF ^{10}Li WITH THE EXPERIMENTAL DATA AND MODEL CALCULATIONS

The data of Table IV are consistent with the experiments of the Amelin group¹² and the group in Michigan.¹⁴ The peak near the maximum proton energy in the reaction $^{11}\text{B}(\pi^-, p)^{10}\text{Li}$ (Ref. 12) (Fig. 5) has width $\leq 0.4 \text{ MeV}$ and covers both levels of the $2^-, 1^-$ doublet of ^{10}Li near the zero of energy. The energy of this peak is $0.15 \pm 0.15 \text{ MeV}$ relative to the neutron threshold of $^{10}\text{Li} \rightarrow ^9\text{Li} + n$. The shift of the

resonance to higher ^{10}Li excitation energies relative to the $2^-, 1^-$ doublet can be attributed to the existence of other ^{10}Li levels in the energy range 0–0.4 MeV above the neutron threshold. Actually, in the reactions $^9\text{Be}(^{13}\text{C}, ^{12}\text{N})^{10}\text{Li}$ at $E_{\text{lab}} = 336 \text{ MeV}$ and $^{13}\text{C}(^{14}\text{C}, ^{17}\text{F})^{10}\text{Li}$ at $E_{\text{lab}} = 337 \text{ MeV}$, Bohlen *et al.*¹⁶ found a 1^+ level at the energy $-0.42 \pm 0.05 \text{ MeV}$ with width $0.15 \pm 0.07 \text{ MeV}$ and a 2^+ level at the energy $-0.80 \pm 0.08 \text{ MeV}$ with width $0.30 \pm 0.10 \text{ MeV}$, corresponding to the level discovered in Ref. 8. Therefore, the resonance in the range 0–0.4 MeV in Ref. 12 covers perhaps the three ($2^-, 1^-, 1^+$), and maybe even the four ($2^-, 1^-, 1^+, 2^+$) lowest levels of ^{10}Li .

The results of Young *et al.* in Michigan should be noted.¹⁴ The high end of the ^8B momentum spectrum in the reaction $^{11}\text{B}(^7\text{Li}, ^8\text{B})^{10}\text{Li}$ ($E_{\text{lab}} = 130 \text{ MeV}$) has two narrow peaks (see Fig. 6), the centroid of which is located at energy $\geq -100 \text{ keV}$ relative to the neutron decay threshold. The width of this doublet structure is estimated to be $\Gamma_{\text{lab}} < 230 \text{ keV}$. These data are in very good agreement with the results of our calculations (see Table IV). The second prominent feature in Fig. 6, to which the authors assigned the energy $-538 \pm 62 \text{ keV}$ above the neutron decay threshold and the width $\Gamma_{\text{lab}} = 358 \pm 23 \text{ keV}$, apparently includes the unresolved $1^+, 2^+$ doublet found in Ref. 16. In the study of Bohlen *et al.*,¹⁶ in the spectra of the reactions $^9\text{Be}(^{13}\text{C}, ^{12}\text{N})^{10}\text{Li}$ (see Fig. 7) and $^{13}\text{C}(^{14}\text{C}, ^{17}\text{F})^{10}\text{Li}$ (Fig. 8) near zero ^{10}Li excitation energy E_x there is a prominent peak, which in both cases covers at least the four lowest levels of ^{10}Li , which are two pairs of doublets with negative ($2^-, 1^-$) and positive ($1^+, 2^+$) parity. These two pairs of levels were resolved in the single experimental study of Young *et al.*¹⁴ In the studies of Amelin *et al.*¹² and Bohlen *et al.*¹⁶ the two pairs of levels are contained within a single peak, and separating them into ($2^-, 1^-$) and ($1^+, 2^+$) groups is quite difficult. The experimental data of the Japanese group at RIKEN (Ref. 13) apparently largely confirm our results and agree with the data of Ref. 16. The experimental data of the American group¹⁵ do not give much information, but they are consistent with our results. Accordingly, the interpretation of the experimental data of Ref. 8 should be reconsidered. The peak of width $\Gamma = 1.2 \pm 0.3 \text{ MeV}$ found in the reaction $^9\text{Be}(^9\text{Be}, ^8\text{B})^{10}\text{Li}$ at $0.80 \pm 0.25 \text{ MeV}$ above the threshold of the decay $^{10}\text{Li} \rightarrow ^9\text{Li} + n$ is simply production, including at least the four $2^-, 1^-$ and $1^+, 2^+$ levels of ^{10}Li .

Careful study of this production (see Fig. 4) on its high-energy side near the neutron threshold reveals a “step” rising above the background, which can be taken to be the contribution of the ($2^-, 1^-$) doublet unresolved experimentally. The main part of the peak apparently describes the ($1^+, 2^+$) doublet, which is also unresolved. There must be at least two of the latter levels in order to explain the variation of the position and width of this pronounced peak in the various reactions studied in Refs. 8 and 12–16. The effect of the ($2^-, 1^-$) levels on the shape and position of the resonance, except at its high-energy tail, can most likely be neglected, as follows from Ref. 14 (see Fig. 6). To be more systematic, in the five sets of experimental data of Refs. 8, 12, 14, and 16 (see Figs. 4–8) it is necessary to subtract the contribution of the ($2^-, 1^-$) levels, using the data of Ref. 14 in order to

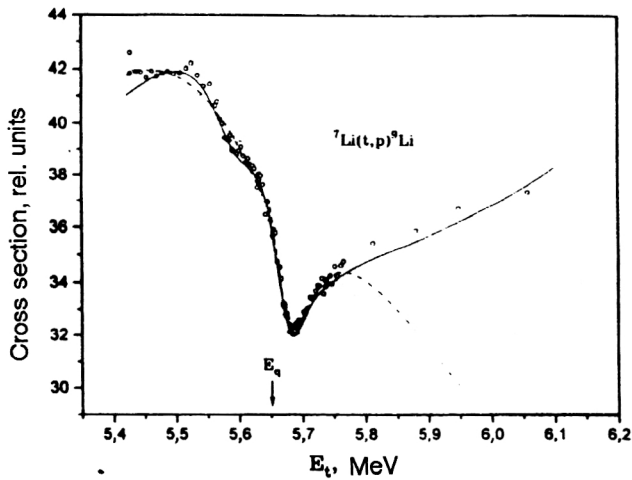


FIG. 9. Experimental data on the cross section (○○○) of the reaction ${}^7\text{Li}(t,p){}^9\text{Li}$ (Ref. 20) near the first threshold of the reaction ${}^7\text{Li}(t,n){}^9\text{Be}^*$ ($T=3/2$) and their approximation on the basis of the theory of threshold phenomena, assuming that in the threshold region there are two states of the ${}^{10}\text{Be}$ nucleus with three possible variants of the parities: $(-, -)$ —solid line, $(+, -)$ —dashed line, and $(+, +)$ —dotted line.

“cleanse” the peak of these levels, and then analyze the cleansed peak as the sum of two peaks in order to determine the position and width of the $(1^+, 2^+)$ doublet. It will probably be necessary with carry out experiments with higher resolution. This is discussed at the end of the review. Let us compare our calculations with the theoretical predictions of the properties of ${}^{10}\text{Li}$ levels in other studies (Refs. 9, 10, 26, 27, and 52). Apparently, the authors of Ref. 9 were the first to point out the possibility of anomalous level population in neutron-rich nuclei. In the ${}^{10}\text{Li}$ nucleus, which has 7 neutrons, in spite of the fact that the number of neutrons is insufficient for totally populating the levels of the $1s$ and $1p$ shells, it is energetically more favorable for the last, seventh neutron to occupy the $2s$ level. As a result of this inverse population the ground state of ${}^{10}\text{Li}$ will have anomalous negative parity instead of the normal positive parity. This conclusion was reached regarding the well known properties of ${}^{11}\text{Be}$, the ground state of which has anomalous positive parity ($\frac{1}{2}^+$) instead of the normal negative parity.

The ${}^{11}\text{Be}$ ground-state configuration is $1s^4 1p^6 2s$, and the structure is that of a ${}^{10}\text{Be}$ core in the ground state plus a $2s$ neutron. The ${}^{11}\text{Be}$ state of lowest normal parity $\frac{1}{2}^-$ with configuration $1s^4 1p^7$ lies at the energy 0.32 MeV (see Fig. 10). For nuclei with $N=7$ and $Z>4$ the lowest levels with normal parity lie below the levels with anomalous parity, and as Z increases the energy spacing grows (see Fig. 10). In the region of ${}^{11}\text{Be}$ the levels first cross, and the ground state has anomalous parity. We have extrapolated this sequence of nuclei to the region $Z<4$ for ${}^{10}\text{Li}$ in our calculations, which gave a ground state with spin and anomalous parity 2^- and configuration $1s^4 1p^5 2s$, and structure of the form of ${}^9\text{Li}$ in the ground state plus a $2s$ neutron. All of this, except for the level energy and the spin of 2, which is not given in Ref. 9, corresponds to the predictions of the authors of that study.⁹ Regarding the lowest level of normal parity, it can be stated that according to the shell-model calculations carried out in

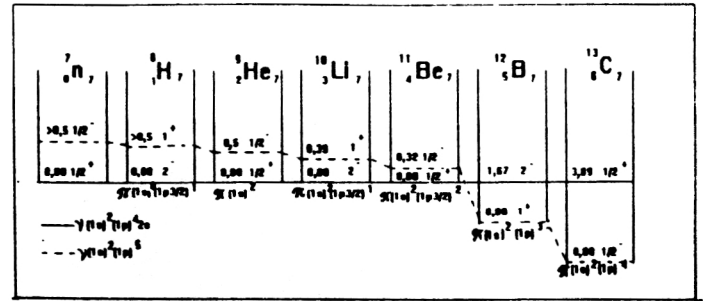


FIG. 10. Systematics of light nuclei for $N=7$ and $Z=0-6$. The energy of the lowest state with anomalous parity is plotted on the horizontal axis. The line of lowest states of “normal” parity (---) crosses the horizontal axis between $Z=4$ and 5.

Refs. 11 and 10 in the $(0+1)\hbar\omega$ model space, the spin and parity are 1^+ , and the energy, in light of the above discussion about the experimental data in reactions with ${}^{10}\text{Li}$ production, is not determined very reliably. We shall use the value $E(1^+)=0.42$ MeV from the neutron threshold, obtained in Ref. 16. The energy interval between the 2^- and 1^+ levels is $0.42-0.027$ MeV ≈ 0.39 MeV, i.e., it is larger than the interval between the lowest levels with anomalous and normal parities in the next nucleus to the right, ${}^{11}\text{Be}$. Therefore, it is observed that these levels tend to move apart for $Z\leq 4$, as they do for $Z>4$ after they cross.

Let us use this systematics to try to predict the properties of the next nucleus with $N=7$ and $Z=2$. It can be assumed that the ${}^9\text{He}$ ground state has spin and parity $\frac{1}{2}^+$ with configuration $1s^4 1p^4 2s$. The structure of the ground state is ${}^8\text{He}(0^+)$ plus a $2s$ neutron. The levels of the nucleon-unstable ${}^9\text{He}$ nucleus have been studied in the reactions ${}^9\text{Be}(\pi^-, \pi^+){}^9\text{He}$ (Ref. 57) and ${}^9\text{Be}({}^{14}\text{C}, {}^{14}\text{O}){}^9\text{He}$ (Ref. 58). The mass excess $\Delta M=40.94(10)$ MeV is determined in Ref. 58 by using the peak with energy 1.27 MeV from the neutron-decay threshold S_n and width $\Gamma\approx 1$ MeV. In Ref. 57 the peak is at a somewhat lower energy, i.e., closer to the neutron threshold: 1.13 ± 0.10 MeV. The neutron orbital angular momentum calculated according to R -matrix theory gives $l=1$ as the most probable value (Ref. 59). It follows from all these data that this resonance production, as in reactions with ${}^{10}\text{Li}$ production, is a conglomerate of several ${}^9\text{He}$ levels of both normal $(-)$ and anomalous $(+)$ parity with intensity of the level (or levels) of negative parity being dominant. The contribution of the ground state of anomalous parity $(+)$ is, according to the systematics of nuclei with $N=7$ (Fig. 10), apparently contained in the step at the low-excitation-energy side of this peak. Owing to the tendency for the lowest levels of anomalous and normal parity to diverge for $Z\leq 4$, for ${}^9\text{He}$ the estimated energy difference between these levels is about 0.5 MeV. Therefore, the ground state of ${}^9\text{He}$ will lie above the threshold for neutron decay ${}^9\text{He}\rightarrow{}^8\text{He}+n$ by ≈ 0.8 MeV (see Fig. 11), which corresponds to the mass excess $\Delta M\approx 40.4$ MeV. The state of ${}^9\text{He}$ of normal parity $(-)$ with energy 1.27 MeV above the neutron decay threshold is apparently the lowest excited state of negative parity. The energies of the ground $\frac{1}{2}^+$ state and the above-mentioned lowest $\frac{1}{2}^-$ state of normal parity will prob-

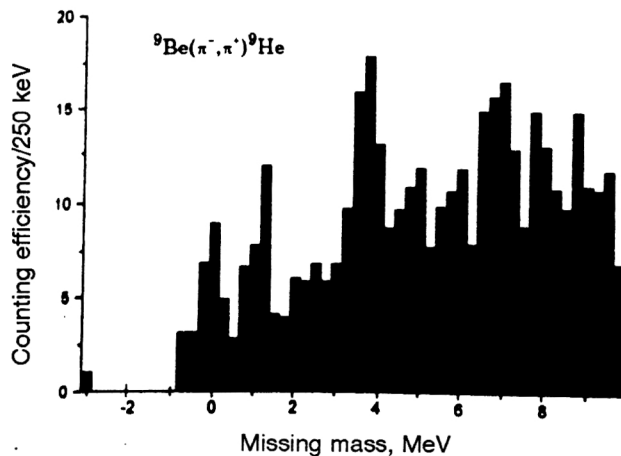


FIG. 11. Spectrum of missing mass in the reaction ${}^9\text{Be}(\pi^-, \pi^+){}^9\text{He}$ for pion energy 180 MeV (Ref. 57) and angle 15° in the lab frame. The ${}^9\text{He}$ mass excess is 1.13 ± 0.10 MeV. The peaks correspond to the excitation energies 0, 1.2, 3.8, and 7.0 MeV.

ably be revised after answering the question of how many levels of both parities are covered by the resonance nearest to the neutron threshold (see Fig. 11).

The ground state of ${}^9\text{He}$ that we predict is absent in Refs. 58 and 59, although it has been calculated by using their experimental data on the basis of systematics of nuclei with $N=7$ (Fig. 10). Let us extend this systematics, assuming that it is valid down to $Z=0$, in order to predict the properties of the nuclei ${}^8\text{H}$ and ${}^7\text{n}$. The ground state of ${}^8\text{H}$ has isospin $T=3$. Analog states with isospin this high for nuclei with $A=8$ have not been studied experimentally. There are also no theoretical calculations, so that there is no approach except systematics. According to it, the ground state of ${}^8\text{H}$ has spin and parity 2^- and configuration $(\pi 1p_{3/2}, \nu 2s_{1/2})$, i.e., owing to the forces pairing it with the odd $2s$ neutron, the single proton of the nucleus has left the $1s$ shell and moved to the $3/2^-$ level of the $1p$ shell. This unexpected effect can be explained as an attempt by the system to increase the nucleon binding energy in order to partially compensate for the neutron mass excess in the nucleus. Whereas in ${}^9\text{He}$ the two protons apparently remain in the $1s$ shell, in ${}^8\text{H}$, where $N/Z=7$, a new qualitative change occurs in the filling of the levels.

The structure of the ${}^8\text{H}$ nucleus can be predicted on the basis of its configuration. Additional criteria that we can use are the Pauli principle, the similarity of wave functions of nucleons of the same shell, and the pairing forces between odd nucleons. According to these criteria, the ground-state structure of the ${}^8\text{H}$ nucleus can be represented as a ${}^6\text{H}(1p^5 2s)$ nucleus plus a dineutron ${}^2\text{n}(1s^2)$ or as a ${}^4\text{H}(1p^3 2s)$ nucleus plus two dineutrons: ${}^2\text{n}(1s^2)$ and ${}^2\text{n}(1p^2)$. The ground state can decay with emission of from one to five neutrons. It is not yet possible to determine the mass excess. From the systematics it can be predicted that the lowest level of normal parity has spin and parity 1^+ and is located >0.5 MeV above the ground state. The prediction of the properties of ${}^7\text{n}$ is even more conservative. The ground state with isospin $T=7/2$ has spin and parity $1/2^+$. The configuration is

$(1s)^2(1p)^4 2s$. Decay with emission of from one to seven neutrons is possible. The mass excess is unknown. The lowest state of normal parity $1/2^-$ apparently has the configuration $(1s)^2(1p)^5$.

Let us conclude this section by comparing the properties of the ${}^{10}\text{Li}$ nucleus that we have found with the theoretical calculations of Refs. 10, 11, 21, 26, 52, and 60. All the shell-model calculations (Refs. 10, 11, 52, and 60) give a ground state of normal parity ($+$). The only difference is in the values of the binding energy and the spin (1 or 2). The value of the spin depends on the version of the model, and the binding energy of the shell model cannot be predicted for the reasons discussed in the method of hyperspherical functions (Sec. 2). In Refs. 52 and 60 the binding energy is described with an accuracy of 0.1 MeV, owing to a specially developed mathematical scheme (see Sec. 2), where the results are fitted to the experimental data. The binding energy of the ${}^{10}\text{Li}$ nucleus is predicted with an accuracy of 0.2 MeV by the empirical Garvey–Kelson relation.²¹ In Ref. 26 the binding energy and parity of the ${}^{10}\text{Li}$ ground state are well described in terms of the experimental value of the lowest $T=2$ level of the stable ${}^{10}\text{B}$ nucleus by using the isobaric-multiplet mass equation.²⁸

Regarding the properties that we predict for ${}^9\text{He}$, the shell-model calculations gave negative parity for the ground state ($1/2^-$) (Refs. 10, 52, and 60) and nucleon instability.

6. DISCUSSION OF THE RESULTS

Let us summarize the review and give some conclusions.

1. At the present time we know of only about ten experimental studies devoted to the ${}^{10}\text{Li}$ nucleus. In them it has been established fairly reliably that the nucleus is unstable to the decay ${}^{10}\text{Li} \rightarrow {}^9\text{Li} + n$ with ground-state decay energy <1 MeV. Several states of ${}^{10}\text{Li}$ have been discovered whose energies, widths, spins, and parities have not been rigorously established up to now. There have been differing, even contradictory, opinions about the level characteristics. It actually has turned out that some data (Refs. 4, 5, 14, and 20) are in fact consistent with others (Refs. 8, 16, and 59), but their interpretation is changed. The broad structure (Refs. 8, 12, 16, 20, and 59) observed near the neutron threshold includes at least four states of the ${}^{10}\text{Li}$ nucleus: the 2^- (g.s.), 1^- doublet and the 1^+ , 2^+ doublet. These two doublets are well resolved in the spectrum in Ref. 14. Moreover, the levels of the 2^- , 1^- doublet also have an obvious splitting (see Fig. 6). Their properties have been established in the present study by analyzing the experimental data of Refs. 4 and 5. The properties of the levels of the 1^+ , 2^+ doublet have not been established definitively: the resolution must be increased in experiments of all types.

2. Theoretical-model calculations are not accurate enough for the reliable prediction of the properties of neutron-enriched nuclei. These methods (including the shell model) have been developed to describe the properties of nuclei in the region $N \approx Z$ and have proved to be not really applicable to exotic nuclei. It is apparently necessary to introduce into the Hamiltonian of the Schrödinger equation a dependence on the excess number of neutrons or different masses of the neutron and proton.

The semiempirical mass formulas (Refs. 21, 28, and 29) based on nuclear systematics have proved to be highly accurate in calculations and in their predictive power (the accuracy of the calculations is <0.1 MeV). The model-independent theory of threshold phenomena (Refs. 17–19, 33, and 34) has proved to be a powerful tool for analyzing the experimental data.^{4,5} The results of this analysis provided answers to key questions about the parity, energy, width, and structure of $T=2$ states of the ^{10}Be nucleus, which are the analogs of the ground state and the first excited state of ^{10}Li . The properties of the analog levels have been extrapolated to the properties of ^{10}Li levels by using the isobaric-multiplet mass equations (IMMEs; Ref. 28).

The model-independent hyperspherical-functions (K -harmonics) method (Refs. 46 and 61), which, it is claimed, can be used to obtain any desired accuracy, is limited on the one hand by the computing power available and, on the other, by the fundamental difficulties in describing the inter-nucleon interaction by means of potential forces. Attempts to avoid these difficulties by introducing an auxiliary basis with fast convergence to a truncated hyperspherical basis and varying the two-particle realistic potential (Refs. 51, 52, and 60) have not given, in our opinion, and cannot give the result desired. The R -matrix method widely used to analyze nuclear reactions is exact (model-independent) at a fundamental level.³⁹ However, the complexity of the method makes it necessary to resort to simplifications or model restrictions, which leads to uncontrolled errors in the calculations. Therefore, the results of the R -matrix analysis (for example, in determining the orbital angular momenta of a resonance⁵⁹) must be treated with care. We note that at present neutron-rich nuclei are being studied near the neutron-decay threshold, where the theory of threshold phenomena¹⁹ is incomparably more effective than any other theory. Its use to analyze experimental data leads most quickly to success.

3. Analog states of the ^{10}Be nucleus with $T=2$ corresponding to levels of the ^{10}Li nucleus have been discovered in the reaction $^7\text{Li}(t,p)^9\text{Li}$ near the neutron threshold of the reaction $^7\text{Li}(t,n)^9\text{Be}^*$ ($E_x=14.3922$ MeV, $J^\pi=\frac{3}{2}^-$, $T=3/2$), owing to the giant threshold anomaly in the integrated cross section. Now we know that the levels corresponding to them in the ^{10}Li nucleus are excited rather weakly in spallation reactions, and they can be discovered only when their location is known (see Figs. 4–8). Therefore, the discovery and study of levels of exotic nuclei and their analogs in isobaric multiplets requires great care and attention, and also techniques of very high resolution. The presence of a nearby neutron threshold greatly simplifies the theoretical analysis for two reasons: (1) the interaction between the level and the threshold state significantly enhances the threshold effect; (2) it may be possible to use the (model-independent) theory of threshold phenomena, which is highly effective in such situations. This theory can be used to determine the parity of a state together with its energy and total width, to calculate or estimate the partial widths, to find the contribution of non-resonance processes, and to determine the coupling of reaction channels. Naturally, it is possible to obtain this much information only when the experimental errors are small,

$\approx 1\%$, when there are enough experimental points in the threshold region $kR < 1$ (number of points greater than the number of theoretical parameters), and when the energy resolution is high, $\Delta E \approx 10$ keV.

Regarding the properties of the first two levels of ^{10}Li (the ground and first excited state), studied here using the theory of threshold phenomena and the analog levels of ^{10}Be , we can state the following. Their parity is negative with probability $>99\%$, and their spins are 2 and 1. It is impossible to rigorously establish the spin sequence from the data on the integrated cross section; the data of the theoretical analysis on the absolute values of the nonresonance part of the amplitudes suggest that the most probable sequence is: 2^- — ^{10}Li ground state, 1^- —first excited state. The ground-state energy is 0.027 ± 0.027 MeV above the threshold of the decay $^{10}\text{Li} \rightarrow ^9\text{Li} + n$. The energy of the first excited state is 0.088 ± 0.043 MeV. The estimated neutron widths are 68 and 14 keV, respectively. They were obtained by assuming equality of the reduced partial widths for tritons and protons in the reaction $^7\text{Li}(t,p)^9\text{Li}$ near the neutron threshold. The ratio of the neutron partial widths is $(\gamma_n^{2^-} / \gamma_n^{1^-})^2 \approx 10$.

The quantum characteristics of the next 1^+ , 2^+ doublet of ^{10}Li are hypothetical; they were obtained by comparing the shell-model calculations¹⁰ and the estimates of the orbital angular momenta⁵⁹ of the peaks, using R -matrix theory. The energies and widths of these states were obtained by representing the observed peak as a sum of two Breit–Wigner resonances.^{16,59} The parameters were determined by variation. They were assigned the following values, measured from the neutron threshold: $S_n = -0.42 \pm 0.05$ MeV for 1^+ and $S_n = -0.80 \pm 0.08$ MeV for 2^+ . The values of the level widths for this doublet are not given in Ref. 16. There it is noted that the authors cannot completely exclude the possibility that the $\nu 2s_{1/2}$ neutron configuration is located below the peak covering the 1^+ , 2^+ doublet. They also suggest that it is possible to hide the $\nu 2s_{1/2}$ configuration under the continuum, owing to the weak excitation and large width. In fact, as we showed above, a configuration of anomalous parity is excited weakly in two narrow levels of ^{10}Li near the zero of S_n at the edge of the strong 1^+ , 2^+ resonance. In Ref. 14 these two weak levels are well separated from the 1^+ , 2^+ states, their centroid is at $S_n \approx -100$ keV, and $\Gamma_{\text{lab}} < 230$ keV. These estimates serve as good proof of the correctness of our calculations of the 2^- , 1^- levels. This is also confirmed by the results of Ref. 12, in which the peak of width of about 1 MeV has a maximum at energy 0.15 MeV, significantly shifted toward the neutron threshold from the center of the 1^+ , 2^+ doublet. This shift can be explained by the fact that the broad resonance covers both the doublets 2^- , 1^- and 1^+ , 2^+ , and in the reaction $^{11}\text{B}(\pi^-, p)^{10}\text{Li}$ the doublet of anomalous parity 2^- , 1^- is excited considerably more strongly than in the reaction $^{11}\text{B}(^7\text{Li}, ^8\text{B})^{10}\text{Li}$ (Ref. 14), and much more strongly than in the reactions $^9\text{Be}(^{13}\text{C}, ^{12}\text{N})^{10}\text{Li}$, $^{13}\text{C}(^{14}\text{C}, ^{17}\text{F})^{10}\text{Li}$ (Ref. 16), and $^9\text{Be}(^9\text{Be}, ^8\text{B})^{10}\text{Li}$ (Ref. 8). Regarding the energy location of the levels of the 1^+ , 2^+ doublet we add the following. In Ref. 14 it was found that the energy centroid of these levels is 538 ± 62 keV from the neutron threshold. The width of the peak encompassing these levels is $\Gamma_{\text{lab}} = 358 \pm 23$ keV. The authors of that study state

TABLE V. Levels of the ^{10}Li nucleus.

E_x , keV	J^π ; T	$\Gamma_{\text{c.m.}}$, keV	$-S_n$, keV	Reaction	Source
0.0 ± 27	$(2)^-, 2$	68	27	$^7\text{Li}(t,p)^9\text{Li}$	here
61 ± 43	$(1)^-, 2$	14	88	- " -	- " -
430	$(1)^+, 2$	≈ 200	460	$^{11}\text{B}(^7\text{Li}, ^8\text{B})^{10}\text{Li}$	Ref. 14
590	$(2)^+, 2$	≈ 200	620	- " -	- " -
2.67 MeV	$(1.0)^-, 2$	< 0.5 MeV	2.7 MeV	$^7\text{Li}(t,p)^9\text{Li}$	Ref. 62
4.02 MeV	$(2)^-, 2$	0.7 ± 0.2 MeV	4.05 MeV	$^9\text{Be}(^{13}\text{C}, ^{12}\text{N})^{10}\text{Li}$	Ref. 16

that if there are two p -wave states in this resonance, they are separated by no more than 160 keV. This is smaller than the value 0.38 MeV quoted in Ref. 16. The positions of states with positive parity in Ref. 14 do not coincide with the data of Ref. 16. In determining the positions of the 1^+ , 2^+ levels we shall use the data of Ref. 14, where the energy resolution is about two times better than in Ref. 16 and is ≈ 70 keV in the excitation energy of the ^{10}Li nucleus. Taking the interval between the 1^+ and 2^+ levels to be 160 keV and their centroid to be located at the resonance energy 538 keV, we obtain $S_n(1^+) = -0.46$ MeV and $S_n(2^+) = -0.62$ MeV. We see that these values differ insignificantly from the data of Ref. 16. We shall insert them into the ^{10}Li level scheme (Table V).

Let us return to discussion of Refs. 4 and 5, in which the integrated cross section of the reaction $^7\text{Li}(t,p)^9\text{Li}$ was measured from threshold to 6 MeV and up to $E_t = 10.5$ MeV in Ref. 20. The two thresholds of the reaction $^7\text{Li}(t,n)^9\text{Be}^*(T=3/2)$ with excitation energy $^9\text{Be}(E_x = 14.3922 \text{ MeV}, J^\pi = \frac{3}{2}^-, \Gamma = 0.381 \text{ keV})$ and $^9\text{Be}(E_x = 16.9752 \text{ MeV}, J^\pi = \frac{1}{2}^-, \Gamma = 0.49 \text{ keV})$ are widely separated. The similarity of these two $^9\text{Be}^*$ states gives rise to similarity of the threshold states of the compound nucleus ^{10}Be which correspond to them. As shown in the present study, near the first threshold the ^{10}Be nucleus has two states with quantum numbers 1^- (below threshold) and 2^- (above threshold) which are analogs of ^{10}Li states. The state above threshold has a large neutron reduced width, close to the one-particle width. It is the analog of the ground state of ^{10}Li lying near the threshold of the decay $^{10}\text{Li} \rightarrow ^9\text{Li} + n$ (27 keV). It is quite probable that the second threshold state studied by us in Refs. 17–19 and 62, which lies ≈ 2.7 MeV above the first state, is in fact a doublet of levels with quantum numbers $0^-, 1^-$. The first above-threshold level must have a large reduced neutron width. This state is the analog of the ^{10}Li state decaying into a neutron and a $^9\text{Li}^*$ nucleus in the first excited state, where the neutron is produced with $l_n = 0$. In Table V we show one level of negative parity with excitation energy 2.7 MeV, since it is not known whether it is a singlet or a doublet. The configuration of this level (or levels) is $(1s)^4(1p)^5(2s)$. The level with energy 4.05 MeV above threshold with the proposed configuration $(1s)^4(1p)^5(1d \frac{5}{2})$ and spin and parity 2^- (Ref. 16) completes the system of levels in Table V.

4. The prediction of the properties of ^9He that we have made here is based on the systematics of nuclei with $N=7$ (Fig. 10) and the experimental data of Refs. 57 and 59. Since this systematics was used in Ref. 9 to correctly predict the properties of the ground state of ^{10}Li , there is no reason for

us not to trust it in the prediction of the properties of the ground state of the nucleus closest in Z , ^9He . Its quantum numbers $\frac{1}{2}^+$ clearly contradict the values $\frac{1}{2}^-$ from the data of Ref. 59, where R -matrix analysis of the state closest to the neutron threshold $^9\text{He} \rightarrow ^8\text{He} + n$ gave $l=1$ as the most probable value. We note that the resonance has width $\Gamma \approx 1$ MeV, and apparently it is the sum of at least two resonances of anomalous ($l=0$) and normal ($l=1$) parity. The ground state with $l=0$ is apparently excited more weakly and gives a smaller contribution to the broad resonance. The lowest state of normal parity ($l=1$) is excited more strongly, and the centroid is shifted toward its location, determined in Refs. 57 and 59 to be in the range 1.13–1.27 MeV. As we have found from the systematics, the energy spacing between these levels is ≈ 0.5 MeV or more. Therefore, the $\frac{1}{2}^+$ ground state of ^9He is located at an energy < 0.8 MeV from the neutron decay threshold, and its total width must be considerably less than 1 MeV. Comparison with the neutron-unstable ^5He and ^7He nuclei shows that they are “incompletely bound” by 0.9 and 0.4 MeV, respectively, and the total widths are 0.6 and 0.16 MeV, i.e., the stability of odd isotopes of He increases with the number of neutrons. Here it is appropriate to note that the Garvey–Kelson relation⁶³ for ^5He and ^7He on the basis of the experimental masses of ^6He and ^8He predicts that the neutron instability of these nuclei grows with increasing mass with incomplete binding by 1.3 and 2.3 MeV, respectively. As far as the systematics of nuclei with $N=7$ is concerned, we guess that it is not unique. Analog systematics can probably exist for nuclei with $N=9, 5$, and so on.

5. Let us conclude with a discussion of new experiments which can improve the available data on the properties of ^{10}Li . At the present time, the experimental techniques in reactions involving π mesons and short-lived nuclei are not sufficiently developed to ensure the desired accuracy, and it is apparently better to study reactions involving stable nuclei at low energies. Examples are the well known reactions $^7\text{Li}(t,p)^9\text{Li}$ and $^7\text{Li}(^3\text{He},p)^9\text{Be}$ with production of the compound nuclei ^{10}Be and ^{10}B of the $A=10$ isobaric-mass multiplet. A very high accuracy of 0.5% and an energy resolution of ≈ 20 keV have been obtained in the measurement of the integrated cross section of the first reaction.⁵ Such high accuracy has not yet been obtained in reactions involving heavy ions. To obtain a more reliable determination of the parity and spin of a compound-nucleus level it is necessary to measure the differential cross sections in addition to the integrated one. The values of the partial widths can be reconstructed from the data on the measurement of the cross sections in all the open channels. The integrated cross sections

for the ${}^7\text{Li}+t$ interaction have been measured (Refs. 4, 5, and 20) in all the reaction channels, along with the differential cross section of elastic scattering.⁶⁴ New experiments to obtain data in channels where they do not conform to the requirements of theoretical analysis will lead to advances both in the determination of the properties of the ${}^{10}\text{Be}$ levels and in the extrapolation of these properties to the other members of the $A=10$ isobaric multiplet, including ${}^{10}\text{Li}$.

¹⁾Deceased.

- ¹A. M. Poskanzer, S. W. Cosper, E. K. Hyde, and J. Cerny, Phys. Rev. Lett. **17**, 1271 (1966).
- ²C. A. Barnes, in *Proc. of the Conf. on Nuclear Isospin*, Asilomar, California (Academic Press, New York, 1969), No. 4, p. 179.
- ³Y. S. Chen, W. D. Harrison, and T. A. Tombrello, Bull. Am. Phys. Soc. **15**, 1598 (1970).
- ⁴S. N. Abramovich, B. Ya. Guzhovskii, A. G. Zvenigorodskii, and S. V. Trusillo, Izv. Akad. Nauk SSSR, Ser. Fiz. **37**, 1967 (1973) [Bull. Acad. Sci. USSR, Phys. Ser.].
- ⁵S. N. Abramovich, B. Ya. Guzhovskii, A. G. Zvenigorodskii, and S. V. Trusillo, Yad. Fiz. **30**, 1276 (1979) [Sov. J. Nucl. Phys. **30**, 665 (1979)].
- ⁶A. Bohr and B. R. Mottelson, *Nuclear Structure*, Vol. 1 (Benjamin, New York, 1969) [Russ. transl., Mir, Moscow, 1971], Chap. 2.
- ⁷F. Ajzenberg-Selove, Nucl. Phys. **A248**, 1 (1975).
- ⁸K. H. Wilcox, R. B. Weisenmiller, G. J. Wozniak *et al.*, Phys. Lett. **59B**, 142 (1975).
- ⁹F. C. Barker and G. T. Hickey, J. Phys. G. **3**, L23 (1977).
- ¹⁰N. A. F. M. Poppelier, L. D. Wood, and P. W. M. Glaudemans, Phys. Lett. **157B**, 120 (1985).
- ¹¹S. Cohen and D. Kurath, Nucl. Phys. **73**, 1 (1965).
- ¹²A. I. Amelin, M. G. Gornov, Yu. B. Gurov *et al.*, Yad. Fiz. **52**, 1231 (1990) [Sov. J. Nucl. Phys. **52**, 782 (1990)].
- ¹³T. Kobayashi, Preprint RIKEN-AF-NP-158, RIKEN (1993); in *Proc. of the Third Intern. Conf. on Radioactive Nuclear Beams*, East Lansing, Michigan, 1993; ${}^{11}\text{Li}+C\rightarrow{}^9\text{Li}+n+X$, $E({}^{11}\text{Li})=72$ MeV/nucleon.
- ¹⁴B. M. Young, W. Benenson, J. H. Kelley *et al.*, *Low-Lying Structure of ${}^{10}\text{Li}$ in the Reaction ${}^{11}\text{B}({}^7\text{Li}, {}^8\text{B}){}^{10}\text{Li}$* (National Superconducting Cyclotron Laboratory and Department of Physics and Astronomy, Michigan State University, East Lansing, Michigan, 1993).
- ¹⁵R. A. Kryger, A. Azhari, A. Galonsky *et al.*, in *Proceedings of the Third Intern. Conf. on Radioactive Nuclear Beams*, East Lansing, Michigan, 1993; ${}^{18}\text{O}+C\rightarrow{}^9\text{Li}+n+X$, $E({}^{18}\text{O})=80$ MeV/nucleon.
- ¹⁶H. G. Bohlen, B. Gebauer *et al.*, Z. Phys. A **344**, 381 (1993).
- ¹⁷S. N. Abramovich, B. Ya. Guzhovskii, A. V. Ershov, and L. M. Lazarev, Izv. Akad. Nauk SSSR, Ser. Fiz. **50**, 2021 (1986) [Bull. Acad. Sci. USSR, Phys. Ser.].
- ¹⁸S. N. Abramovich, B. Ya. Guzhovskii, A. V. Ershov, and L. M. Lazarev, Yad. Fiz. **46**, 499 (1987) [Sov. J. Nucl. Phys. **46**, 269 (1987)].
- ¹⁹S. N. Abramovich, B. Ya. Guzhovskii, and L. M. Lazarev, Fiz. Elem. Chastits At. Yadra **23**, 305 (1992) [Sov. J. Part. Nucl. **23**, 129 (1992)].
- ²⁰S. N. Abramovich, B. Ya. Guzhovskii, S. A. Dunaeva, A. G. Zvenigorodskii, and S. V. Trusillo, Vopr. At. Nauki Tekh. (Ser. Yad. Konstanty) No. 2, 14 (1985) [in Russian].
- ²¹N. A. Jelley, J. Cerny, D. P. Stahel, and K. H. Wilcox, Phys. Rev. C **11**, 2049 (1975).
- ²²T. Kobayashi, O. Yamakawa, and K. Omata, Phys. Rev. Lett. **60**, 2599 (1988).
- ²³F. Ajzenberg-Selove, Nucl. Phys. **A506**, 1 (1990).
- ²⁴I. Tanihata, Nucl. Phys. **A478**, 795c (1988).
- ²⁵M. G. Saint-Laurent *et al.*, Z. Phys. A **332**, 457 (1989).
- ²⁶E. K. Warburton and B. A. Brown, Phys. Rev. C **46**, 923 (1992).
- ²⁷A. G. M. van Hees and P. W. M. Glaudemans, Z. Phys. A **314**, 323 (1983); **315**, 223 (1984).
- ²⁸M. S. Antony, J. Britz, J. B. Bueb, and A. Pape, At. Data Nucl. Data Tables **33**, 447 (1985).
- ²⁹E. P. Wigner, in *Proc. of the Robert A. Welch Foundation Conf. on Chemical Research*, edited by W. O. Milligan, Houston, 1958, Vol. 1, p. 88.
- ³⁰J. Janecke, Phys. Rev. **147**, 735 (1966); in *Isospin in Nuclear Physics*, edited by D. H. Wilkinson (North-Holland, Amsterdam, 1969), p. 297.
- ³¹E. M. Henley and C. E. Lacy, Phys. Rev. **184**, 1228 (1969).
- ³²G. T. Garvey, *Nuclear Isospin*, edited by J. D. Anderson, S. D. Bloom, J. Cerny, and W. W. True (Academic Press, New York, 1969), p. 703.
- ³³L. M. Lazarev, Izv. Akad. Nauk SSSR, Ser. Fiz. **51**, 171 (1987) [Bull. Acad. Sci. USSR, Phys. Ser.].
- ³⁴L. M. Lazarev, Ukr. Fiz. Zh. **36**, 661 (1991) [in Russian].
- ³⁵E. P. Wigner, Phys. Rev. **73**, 1002 (1948).
- ³⁶G. Breit, Phys. Rev. **107**, 1612 (1957).
- ³⁷A. I. Baz', Ya. B. Zel'dovich, and A. M. Perelomov, *Scattering, Reactions and Decay in Nonrelativistic Quantum Mechanics*, transl. of 1st Russ. ed. (Israel Program for Scientific Translations, Jerusalem, 1966) [Russ. original, 2nd ed., Nauka, Moscow, 1971], Chap. IX.
- ³⁸N. Jarmie, R. E. Brown, and R. A. Hardekopf, Phys. Rev. C **29**, 2031 (1984); R. E. Brown, N. Jarmie, and G. M. Hale, Phys. Rev. C **35**, 1999 (1987); Phys. Rev. Lett. **59**, 763 (1987).
- ³⁹A. M. Lane and R. G. Thomas, Rev. Mod. Phys. **30**, 257 (1958) [Russ. transl., IL, Moscow, 1960].
- ⁴⁰L. M. Lazarev, in *Abstracts of Reports Presented at the Forty-Fourth Intern. Meeting on Nuclear Spectroscopy and Nuclear Structure* [in Russian], St. Petersburg, 1994 (Nauka, St. Petersburg, 1994), p. 234.
- ⁴¹G. F. Filippov and I. P. Okhrimenko, Yad. Fiz. **32**, 932 (1980) [Sov. J. Nucl. Phys. **32**, 480 (1980)]; **33**, 928 (1981) [**33**, 488 (1981)].
- ⁴²H. M. Hoffman, Nucl. Phys. **A416**, 363 (1984).
- ⁴³E. W. Schmid and H. Ziegelmann, *The Quantum Mechanical Three-Body Problem* (Pergamon Press, Oxford, 1974) [Russ. transl., Nauka, Moscow, 1979].
- ⁴⁴A. B. Volkov, Nucl. Phys. **74**, 33 (1965).
- ⁴⁵F. Tanabe, A. Tashaki, and R. Tamagaki, Prog. Theor. Phys. **53**, 677 (1975).
- ⁴⁶Yu. A. Simonov, Yad. Fiz. **3**, 630 (1966) [Sov. J. Nucl. Phys. **3**, 461 (1966)]; **7**, 1210 (1968) [**7**, 722 (1968)]; E. L. Surkov, Yad. Fiz. **5**, 908 (1967) [Sov. J. Nucl. Phys. **5**, 644 (1967)].
- ⁴⁷M. V. Zhukov, B. V. Danilin, D. V. Fedorov *et al.*, Phys. Lett. B **265**, 19 (1991).
- ⁴⁸H. Mang and H. Weidenmüller, Ann. Rev. Nucl. Sci. **18**, 1 (1968).
- ⁴⁹H. Eickmeier and H. H. Hackenbroich, Nucl. Phys. **A169**, 407 (1971).
- ⁵⁰R. Bryan and B. L. Scott, Phys. Rev. **135**, 434 (1964); **164**, 1215 (1967); **177**, 1435 (1969).
- ⁵¹A. M. Gorbato, Yu. N. Krylov, and A. B. Solov'ev, Yad. Fiz. **29**, 866 (1979) [Sov. J. Nucl. Phys. **29**, 445 (1979)].
- ⁵²A. M. Gorbato, V. L. Skopich, P. Yu. Nikishov, and Yu. É. Penionzhkevich, Yad. Fiz. **50**, 1551 (1989) [Sov. J. Nucl. Phys. **50**, 962 (1989)].
- ⁵³D. Gogny, P. Pires, and R. de Tourel, Phys. Lett. **32B**, 591 (1970).
- ⁵⁴F. Calogero and Yu. A. Simonov, Nuovo Cimento **64B**, 337 (1969).
- ⁵⁵V. K. Grishin, F. A. Zhivopistsev, and V. A. Ivanov, *Mathematical Analysis and Interpretation of Physics Experiments* [in Russian] (Moscow State University Press, Moscow, 1988).
- ⁵⁶F. Ajzenberg-Selove, Nucl. Phys. **A490**, 1 (1988).
- ⁵⁷K. K. Seth, M. Artuso, D. Barlow *et al.*, Phys. Rev. Lett. **58**, 1930 (1987).
- ⁵⁸H. G. Bohlen, Z. Phys. A **330**, 227 (1988).
- ⁵⁹H. G. Bohlen, B. Gebauer, M. von Locke-Petsch *et al.*, in *Proc. of the Intern. School-Seminar on Heavy Ion Physics* [in Russian], edited by Yu. Ts. Oganessian, Yu. E. Penionzhkevich, and R. Kalpakchieva, Dubna, 1993, Vol. 1, p. 17.
- ⁶⁰A. M. Gorbato, P. Yu. Nikishov, V. L. Skopich *et al.*, in *Proc. of the Intern. School-Seminar on Heavy Ion Physics* [in Russian], edited by Yu. Ts. Oganessian, Yu. E. Penionzhkevich, and R. Kalpakchieva, Dubna, 1993, Vol. 1, p. 54.
- ⁶¹A. I. Baz', V. F. Demin, and M. V. Zhukov, Fiz. Elem. Chastits At. Yadra **6**, 515 (1975) [Sov. J. Part. Nucl. **6**, 207 (1975)].
- ⁶²B. Ya. Guzhovskii and L. M. Lazarev, Izv. Akad. Nauk SSSR, Ser. Fiz. **54**, 2250 (1990) [Bull. Acad. Sci. USSR, Phys. Ser.].
- ⁶³G. T. Garvey and I. Kelson, Phys. Rev. Lett. **16**, 197 (1966); G. T. Garvey *et al.*, Rev. Mod. Phys. **41**, 51 (1969).
- ⁶⁴S. N. Abramovich, B. Ya. Guzhovskii, B. M. Dzyuba *et al.*, in *Problems in Nuclear Physics and Cosmic Ray Particles*, Vishcha Shkola, Khar'kov, 1977, No. 7, p. 41 [in Russian].

Translated by Patricia A. Millard